frontiers | Frontiers in Earth Science

TYPE Original Research
PUBLISHED 25 November 2022
DOI 10.3389/feart.2022.988373

OPEN ACCESS

EDITED BY
Marco Neri,
National Institute of Geophysics and Volcanology, Italy

REVIEWED BY
Yasui Maya,
Nihon University, Japan
Claudio Scarpati,
University of Naples Federico II, Italy

*CORRESPONDENCE
Ayumu Nishihara,
172s415s@gsuite.kobe-u.ac.jp

SPECIALTY SECTION
This article was submitted to Volcanology, a section of the journal Frontiers in Earth Science

RECEIVED 07 July 2022
ACCEPTED 18 October 2022
PUBLISHED 25 November 2022

CITATION
Nishihara A, Geshi N and Naruo H (2022), Long-term change of the eruption activities of Sakurajima volcano, Japan, inferred from the fallout tephra deposits.
Front. Earth Sci. 10:988373.
doi: 10.3389/feart.2022.988373

Long-term change of the eruption activities of Sakurajima volcano, Japan, inferred from the fallout tephra deposits

Ayumu Nishihara[1,2]*, Nobuo Geshi[2] and Hideto Naruo[3]

[1]Department of Planetology, Graduate School of Science, Kobe University, Kobe, Japan, [2]Geological Survey of Japan (AIST), Tsukuba, Japan, [3]Board of Education, Aira Municipal Government, Aira, Japan

Stratigraphic analysis of fallout tephra deposits in and around a volcano provides a framework for understanding the long-term temporal change in the volcano's activities. Here, we reconstruct the evolution of the volcanic activities of Sakurajima volcano based on reconstructed tephra stratigraphy by original field surveys, compilations of geological and archeological data, and new ^{14}C dating. We define three eruption stages of Stage 1 (30–24 ka), Stage 2 (12.8–4.8 ka), and Stage 3 (4.5 ka–present), based on a major hiatus and shifting of the volcanic centers. Stages 2 and 3 are further subdivided according to the predominant mode of volcanic activity. Revised distribution of tephra deposits indicates that a total of 14.5 km^3 (5.8 km^3 dense rock equivalent) of fallout tephra has erupted from Sakurajima. Among them, Stage 2a (13–8 ka) produced the largest volume of tephra fallout deposits, suggesting that Sakurajima peaked in magma discharge during Stage 2a (2.9 km^3/kyr) and then decreased rapidly toward Stage 2b (8–4.8 ka; 0.07 km^3/kyr). The eruption of large-volume tephra deposits in Stage 2a, followed by the development of a thick volcanic ash layer in Stage 2b, indicates the eruption style shifted from explosive pumice eruptions in Stage 2a to ash-producing Vulcanian activity in Stage 2b, with decreasing magma discharge rate. Thick volcanic ash deposits covered by several fallout tephra deposits during Stage 3 also reflect a shift in activity from repeated Vulcanian explosions with lava effusions in Stage 3a (4.5–1.6 ka) to predominantly pumice eruptions during the historical period (Stage 3b) with an increasing magma discharge rate. The case study of Sakurajima presented here demonstrates that the combined analysis of the distribution, stratigraphy, and age of pumice fall layers with the lava and pyroclastic cone deposits on the volcanic edifice is a powerful tool for deciphering the growth history of complex stratovolcanoes.

KEYWORDS

Sakurajima volcano, stratigraphic analysis, fallout tephra deposit, tephra volume, ^{14}C dating, eruptive history, volcanic edifice growth

Introduction

Detailed geological examinations of eruption histories are a high-priority research objective for evaluating the current status and forecasting the future behavior of active volcanoes (Yamamoto et al., 2018). In order to fully understand the eruption history of volcanoes, analysis of proximal lavas and pyroclasts, ejecta from relatively small-scale eruptive activities, and fallout tephra and large-scale pyroclastic flow deposits distributed over a wide area should be integrated (e.g., Zernack et al., 2011; Leonard et al., 2021).

Fallout tephra deposits in areas far from a volcano are important records of the history of volcanic activity because the ejecta deposited around the vent erupted during its early stages are covered by subsequent ejecta or eroded out from the edifice (e.g., Allan et al., 2008; Sunyé-Puchol et al., 2022). The stratigraphic relationships, ages, and volumes of fallout tephra deposits constrain the evolution of explosive activities at a volcano (e.g., Donoghue et al., 1995; Miyabuchi, 2009). Developments in dating techniques (e.g., ^{14}C dating and paleomagnetic secular variation) have enabled improvements to the precision and resolution of volcanic activity reconstructions (e.g., Greve and Turner, 2017; Obrochta et al., 2018). Systematic compiling of each tephra layer's characteristics (distribution, volume, composition, internal structure, and petrologic features) will reveal the volcano's evolution and its magma plumbing system (e.g., Óladóttir et al., 2008; Geshi et al., 2022). For this purpose, detailed field surveys that span proximal to distal areas of volcanoes represent valuable contributions.

Sakurajima volcano in southwest Japan provides an ideal target for investigating the high-resolution history of an active volcano using the geological analysis of fallout tephra. At least seventeen pumice fall deposits have been known during Sakurajima's history (e.g., Fukuyama, 1978; Moriwaki, 1994; Kobayashi et al., 2013). Here, we reconstructed the stratigraphic relationship of Sakurajima's major pumice fall deposits based on our detailed field survey and compilation of geological and archeological data. Based on the tephra stratigraphy, we try the reconstruction of the growth of the volcano.

Sakurajima volcano

Geological background

Sakurajima is an active volcano of the southwestern Japan Arc, formed by the subduction of the Philippine Sea plate beneath the Eurasia plate at the Ryukyu trench. Sakurajima volcano is located in the southern part of Kyushu Island, where six large calderas younger than ~0.6 Ma (Kakuto, Kobayashi, Aira, AtaN, AtaS, and Kikai calderas) and two smaller calderas (Wakamiko and Ikeda calderas) align in a volcano-tectonic graben (Kagoshima graben; Tsuyuki, 1969) along the volcanic front (Figure 1A).

Sakurajima is one of the post-caldera volcanoes of Aira caldera (Matumoto, 1943), which was shaped by a 30 ka supereruption (Aramaki, 1984; Smith et al., 2013). The age of the lavas and tephra at the base of the Sakurajima deposits suggest that the volcanic activities of Sakurajima commenced around the present location of Kitadake after the 30 ka supereruption (Uto et al., 1999; Miki et al., 2000; Okuno, 2002).

Sakurajima volcano's present edifice comprises two major stratovolcanic edifices (Kitadake and Minamidake) aligned from north ("kita" in Japanese) to south ("minami" in Japanese). The structural relationship between the two edifices indicates that the formation of the volcanic edifice of Minamidake followed the growth of Kitadake. Several lateral cones and lava domes are distributed on the flank of the Sakurajima edifice. Kitadake has a single summit crater of 500 m in diameter, and Minamidake has two summit craters (Minamidake summit crater (M) and Showa(S) crater in Figure 1B).

Most of the lavas and tephra of Sakurajima have an andesitic-dacitic composition (Takahashi et al., 2013; Geshi et al., 2020). Wakamiko produced several rhyolitic ejecta (Kano et al., 1996; Nishimura and Kobayashi, 2015; Kano et al., 2022).

Eruption stages

We have broadly defined three eruption stages, "Stage 1, 2, 3," in order from oldest to youngest, based on a major hiatus and shifts in the loci of volcanic centers. The three stages correspond to the Older-Kitadake stage, the Younger-Kitadake stage, and the Older-Minamidake and Younger-Minamidake stages defined by Kobayashi et al. (2013). Stages 2 and 3 were further subdivided according to the predominant mode of volcanic activity.

The volcanic activities of the three eruption stages are summarized in Figure 2. Seventeen pumice fall deposits that erupted during the active period of Sakurajima have been identified (Kobayashi et al., 2013). The Sakurajima tephra deposits have different names due to differences in nomenclature. One is to name each tephra in stratigraphic order (Fukuyama, 1978; Kobayashi, 1986b), and the other is to name tephras after the type localities (Moriwaki, 1990; Moriwaki, 1994). In addition, some tephra deposits have local names used in regional areas (e.g., Soda, 1997). In this paper, the nomenclature of the Sakurajima tephra deposits follows Kobayashi (1986b), which are named P17 to P1 from lower to higher levels. The correspondence of each tephra name is summarized in Supplementary Table S1.

Stage 1 is the first volcanic stage of Sakurajima (30–24 ka), just after the 30 ka supereruption. At least three pumice-bearing explosive eruptions forming P17, P16, and P15 tephra deposits occurred during 26–24 ka (Kobayashi, 1986b; Kobayashi, 1989; Okuno, 2002). Some lavas from the Sakurajima basement have been dated to Stage 1 (Uto et al., 1999; Miki et al., 2000), suggesting lava effusions also occurred during Stage 1.

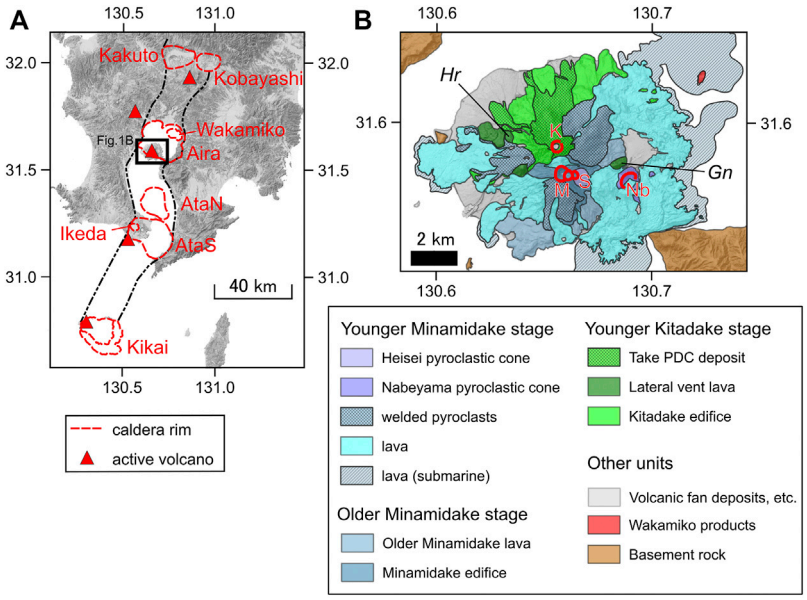

FIGURE 1
(A) Distribution of active volcanoes (red triangles) defined by Japan Meteorological Agency, and calderas (broken red lines) younger than ~0.6 Myr, in southern Kyushu. The topographic rims of each caldera are defined after Machida et al. (2001), Kobayashi et al. (2013), and Tatsumi et al. (2018). The dashed-and-dotted lines along the north-south direction represent "Kagoshima graben" (Tsuyuki, 1969). Two smaller calderas (Wakamiko and Ikeda caldera) nest within larger calderas (Aira and AtaS calderas, respectively). The GSI Maps (Shaded Map and Slope Map; https://maps.gsi.go.jp/development/ichiran.html) published by Geospatial Information Authority of Japan are used as the background maps. **(B)** Geological map of Sakurajima volcano (modified from Kobayashi et al., 2013). Red lines represent crater rims described in Kobayashi et al. (2013). Abbreviations of the craters are the followings; K: Kitadake, M: Minamidake, S: Showa, Nb: Nabeyama. The italic characters of Hr and Gn represent the name of Kitadake flank lavas, Harutayama and Gongenyama lavas, respectively (see Figure 2). The GSI Maps (Shaded Map and Slope Map; https://maps.gsi.go.jp/development/ichiran.html) published by Geospatial Information Authority of Japan are used as the background maps.

Stage 2 is defined as activities between 12.8 and 4.8 ka (Kobayashi, 1989; Kobayashi et al., 2013). The volcanic center of Stage 2 is around the Kitadake edifice, which produced several explosive and effusive eruptions (Kobayashi et al., 2013). This stage is characterized by a series of pumice eruptions, which produced at least ten pumice fall deposits (P14-P5 tephra deposits; Kobayashi, 1989; Kobayashi and Ezaki, 1997). Eight (P14-P11, P8-P5) pumice fall deposits can be traced outside of Sakurajima Island, and the others (P10, P9 tephras) are observed only on an outcrop inside Sakurajima Island (Kobayashi, 1986b). The eruption age of the Kitadake lava in the northern Kitadake edifice, which comprises the main component of the Kitadake body, is estimated to be 10.5–9.5 ka based on K-Ar and paleomagnetic data (Sudo et al., 2001; Miki et al., 2003; Uto et al., 2005). The stratigraphic relationship between the pumice fall deposits and Gongenyama lava (Gn in Figure 1B), which is distributed on the eastern flank of Kitadake, indicates that the Gongenyama lava erupted before 8 ka. The eruption age of Harutayama lava (Hr in Figure 1B) distributed on the western flank of Kitadake is estimated to be 7 or 9 ka based on paleomagnetic data (Miki et al., 2000; Uto et al., 2005). The other flank lavas are considered to have erupted at about the same time as the Harutayama and Gongenyama lavas due to similar chemical characteristics (Miki et al., 2003; Kobayashi et al., 2013; Takahashi et al., 2013). A pyroclastic density current deposit discharged by the P5 eruption (called Take tephra deposits), the last eruption of Stage 2, is widely distributed on the northern flank of the Kitadake edifice (Figure 1B; Kobayashi, 1986b; Hiramine et al., 2015).

Stage 3 includes the volcanic activities that have occurred at the volcanic center around the Minamidake edifice. Stage 3 subdivides into two eruption stages, "Stage 3a and 3b," corresponding to the Older-Minamidake and the Younger-Minamidake stages defined by Kobayashi et al. (2013).

Stage 3a covers activities at Minamidake from 4.5 to 1.6 ka, characterized by ash ejections and lava effusions (Kobayashi, 1986a; Miki and Kobayashi, 2016). No major pumice fall deposit is known at this stage (Kobayashi et al., 2013). The thick ash deposits called "Minamidake Volcanic Sand (MVS)" are the products of repeated Vulcanian eruptions and are distributed around Sakurajima Island (Kobayashi, 1986a). The Miyamoto, Kannonzaki, and Arimura lavas on the southern flank of Minamidake and the Kurokamigawa lava on the eastern flank erupted during this stage (Miki and Kobayashi, 2016).

Stage 3b represents Sakurajima's current volcanic stage, which started in AD 764. Four historical pumice eruptions

have occurred (Kobayashi, 1982; Kobayashi et al., 2013). All four eruptions occurred from the flank of the Minamidake edifice and discharged pumice clasts accompanied by lava effusions (Kobayashi, 1982; Miki, 1999). The latest pumice eruption occurred in AD 1914. During this stage, several lava effusions also occurred around the summit of Minamidake (Kobayashi et al., 2009; Kobayashi, 2010; Miki et al., 2012). The Showa crater was formed by an explosive eruption in AD 1939 and effused lava in AD 1946 without discharging pumice clasts. After a 9-year hiatus, repeated small-scale Vulcanian eruptions have continued from AD 1955 to the present and formed the Heisei pyroclastic cone near the summit of the Minamidake edifice (Kobayashi et al., 2013).

Methods

Reconstruction of the distribution and stratigraphy of the pumice fall deposits were conducted based on our original field survey and by compiling previous datasets, as the tephra sequence of Sakurajima has been studied from geological and archeological interests.

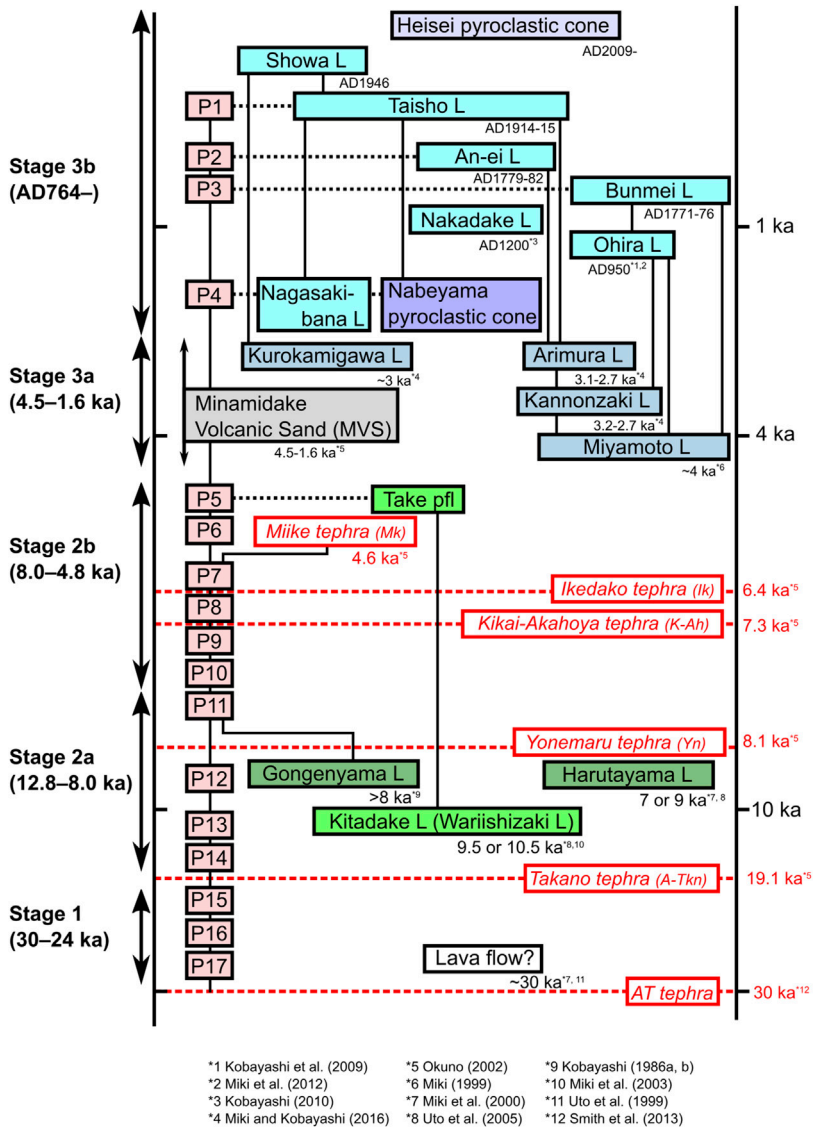

FIGURE 2
The sequence of the eruptive products of Sakurajima volcano. Abbreviations of "L" represent "lava." The solid colors of each lava are identical to Figure 1B. Tephra deposits shown in red are the exotic ones interbedding within the Sakurajima tephra. Dotted black horizontal lines represent volcanic products produced by a single eruption with several phases. Solid black vertical lines indicate that the sequence relationships of the two products connected by the lines have been confirmed.

We surveyed the tephra distribution in and around Sakurajima and measured the thickness of its pumice fall deposits at 65 outcrops (Figure 3A). Figure 3B shows columnar sections of representative outcrops observed with the stratigraphic relationship of the pumice fall deposits (Table 1). Representative stratigraphical relationships of Sakurajima tephra are shown in Figures 4A–F. All data of Sakurajima tephra thickness measured in this study are listed in Supplementary Table S2.

Many previous studies reported the distribution of the thickness of the pumice fall deposits of Sakurajima (Kanai, 1920; Iwamatsu and Kobayashi, 1984; Kobayashi, 1986a;

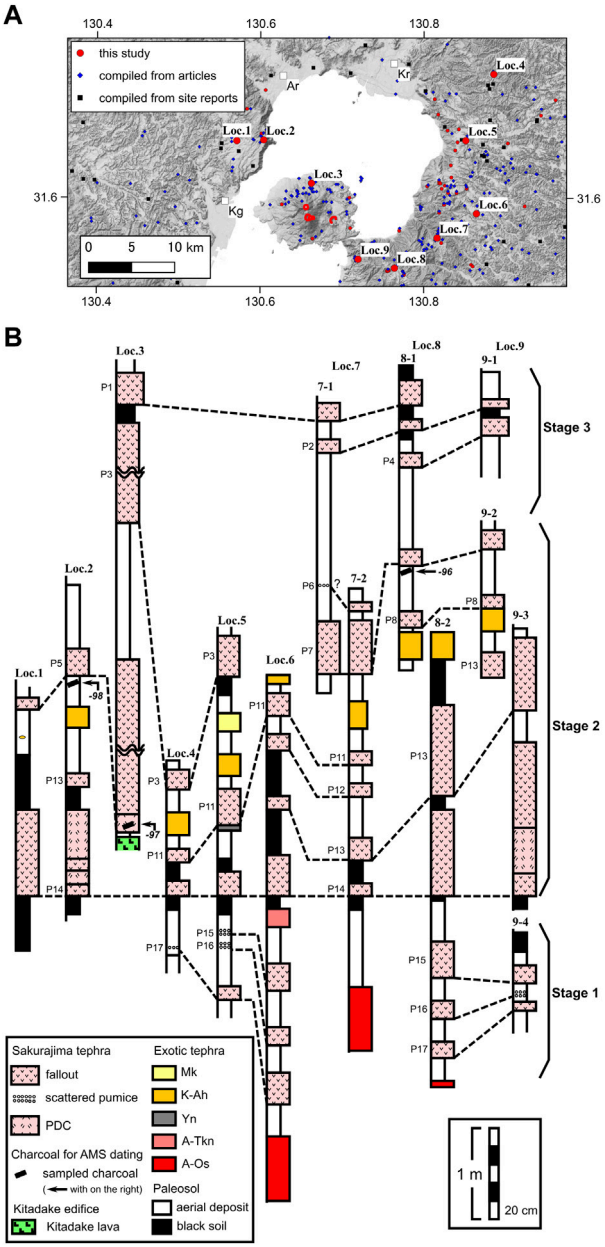

FIGURE 3
(A) Localities of outcrops (solid red circles) around the Sakurajima volcano described in this study. The GSI Maps (Shaded Map and Slope Map; https://maps.gsi.go.jp/development/ichiran.html) published by Geospatial Information Authority of Japan are used as the background maps. **(B)** Representative columnar sections of Sakurajima volcano. Localities of the sections are described in Figure 3A and listed in Table 1. The numbers accompanying the charcoal are the last two digits of the Lab No. of the ^{14}C dated sample (Table 2). The abbreviations of exotic tephras are the followings: Mk, Miike tephra; K-Ah, Kikai-Akahoya tephra; Yn, Yonemaru tephra; A-Tkn, Takano tephra; A-Os, Osumi pumice fall deposit which is a part of AT tephra.

TABLE 1 Localities of the representative outcrops which can confirm the stratigraphic relationships of Sakurajima tephra deposits. The abbreviations of exotic tephras are the followings: Mk, Miike tephra; K-Ah, Kikai-Akahoya tephra; Yn, Yonemaru tephra; A-Tkn, Takano tephra; A-Os, Osumi pumice fall deposit which is a part of AT tephra.

Locality in Figure 2		Latitude	Longitude	Distance from Kitadake crater (km)	Exposed tephra deposits	
					Sakurajima tephra	exotic tephra
Loc.1		31.65996	130.571	11.1 NW	P5, P14	K-Ah
Loc.2		31.66088	130.6039	9.2 NNW	P5, P13, P14	K-Ah
Loc.3		31.61556	130.6624	2.8 NNE	P1, P3, P5	
Loc.4		31.73017	130.8854	26.7 NE	P3, P11, P14, P17?	K-Ah
Loc.5		31.66052	130.8512	20.1 ENE	P3, P11, P14-P17	Mk, K-Ah, Yn
Loc.6		31.58386	130.8643	19.8 E	P11-P17	A-Tkn? A-Os
Loc.7	7–1	31.55827	130.8161	15.6 ESE	P1, P2, P6? P7	
	7–2	31.553	130.8213	16.2 ESE	P6, P7, P11-P14	K-Ah, A-Os
Loc.8	8–1	31.52667	130.7642	12.5 SE	P1, P2, P4, P7, P8	K-Ah
	8–2	31.52389	130.7572	12.1 SE	P13-P17	K-Ah, A-Tkn? A-Os
Loc.9	9–1	31.53583	130.7197	8.6 SE	P2, P4	K-Ah
	9–2	31.53713	130.7165	8.3 SE	P7, P8, P13	
	9–3	31.53606	130.7196	8.5 SE	P13, P14	
	9–4	31.53611	130.7186	8.8 SE	P15-P17	

Kobayashi, 1986b; Kobayashi, 1989; Moriwaki, 1994; Kobayashi and Ezaki, 1996; Inoue et al., 1997; Kagoshima Prefecture, 1999; Kobayashi and Tameike, 1999; Nagasako et al., 1999; Okuno et al., 1999; Kobayashi and Tameike, 2002; Moriwaki, 2010; Moriwaki et al., 2011; Tsukui, 2011; Kobayashi et al., 2013; Yamamoto et al., 2013; Hiramine et al., 2015; Moriwaki et al., 2015; Ikuta et al., 2016; Moriwaki et al., 2017; Todde et al., 2017; Sagawa et al., 2018; Kuwahata et al., 2021; Sun et al., 2021; Hayashida et al., 2022; Kano et al., 2022). As most of the outcrops reported in these previous studies have been destroyed and lost, we used the thickness data from these publications. In this study, the occurrences of tephra deposits were compiled from the cited literature without our evaluation. The localities of the outcrops were determined using QGIS software from the printed distribution maps in cases where they did not provide the latitude/longitude information. The thickness of the pumice fall deposits was extracted by columnar sections described in each article, using the web-based measurement tool to extract data from images (WebPlotDigitizer ver. 4.4; https://automeris.io/WebPlotDigitizer). The detailed compiled information on each tephra that was obtained from the literature is shown in Supplementary Table S3. Furthermore, the Sakurajima tephra deposits have an important role as a chronological indicator in archeological studies (Moriwaki et al., 2016, and reference therein). We also extracted tephra descriptions from the reports of archeological sites because, locally, some tephra are exposed in archeological excavations. The dataset of the archeological site report is summarized in Nishihara et al. (2022).

We determined the ^{14}C age of three charcoal samples from three outcrops to determine the ages of P5 and P7 tephra deposits. The sampling positions of the charcoal are shown in Figure 3B. Sample 211117A-C01 is a small (<3 mm) fragment of charcoal collected from the paleosol 5 cm below the base of the P7 pumice fall deposit. The sample 211115E-C03 is a small piece of rod-shaped charcoal in pumiceous ash at the base of the PDC deposit of the P5 tephra. Sample 211114C-C02 is small fragments of charcoal scattered in the paleosol <5 cm below the base of the P5 pumice fall deposit.

The ^{14}C ages were determined by Accelerator Mass Spectrometry (AMS) method. The sample preparation and the AMS ^{14}C dating were performed at the Institute of Accelerator Analysis Limited. All ^{14}C ages were calibrated using OxCal v4.4 (Ramsey, 2009) and the IntCal20 calibration curve (Reimer et al., 2020).

Distribution, stratigraphy, and age of tephra deposits

The term "tephra" includes non-welded pyroclastic fall and flow deposits (e.g., Lowe and Hunt, 2001, and reference therein). In the following, the term "pumice fall deposit" refers only to pyroclastic fallout deposits mainly comprising pumice and ash particles, and the term tephra deposit is used to refer to a series of deposits that also include some pyroclastic flow deposits. Here, we identify an aerial deposit as a paleosol beneath tephra unit which is a clayey

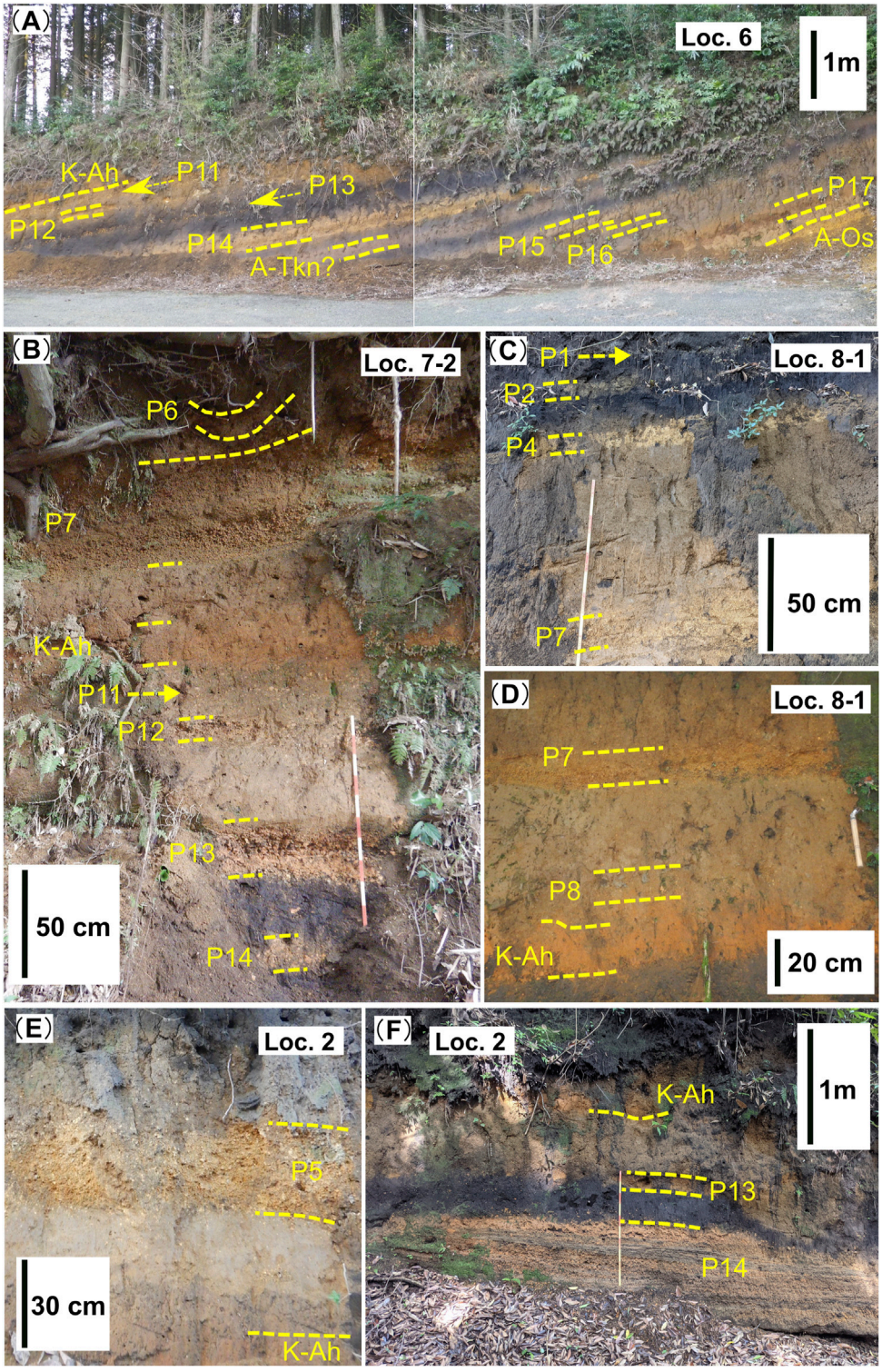

FIGURE 4
(A) Stratigraphic relationship of tephra deposits during Stage 1 and Stage 2 at Loc. 6, 19.8 km east of the Kitadake summit crater. In this outcrop, a stratigraphical relationship between the P17-P11 tephra deposits is observed with some exotic tephras. **(B)** Stratigraphic relationship of tephra deposits during Stage 2 at Loc. 7–2, 16.2 km southeast of the Kitadake summit crater. **(C,D)** Stratigraphic relationship of tephra deposits during Stage 2 and Stage 3. At Loc. 8–1, 12.5 km southeast of the Kitadake summit crater. **(E,F)** Stratigraphic relationship of tephra deposits during Stage 2 at Loc. 2, 9.2 km northwest of the Kitadake summit crater.

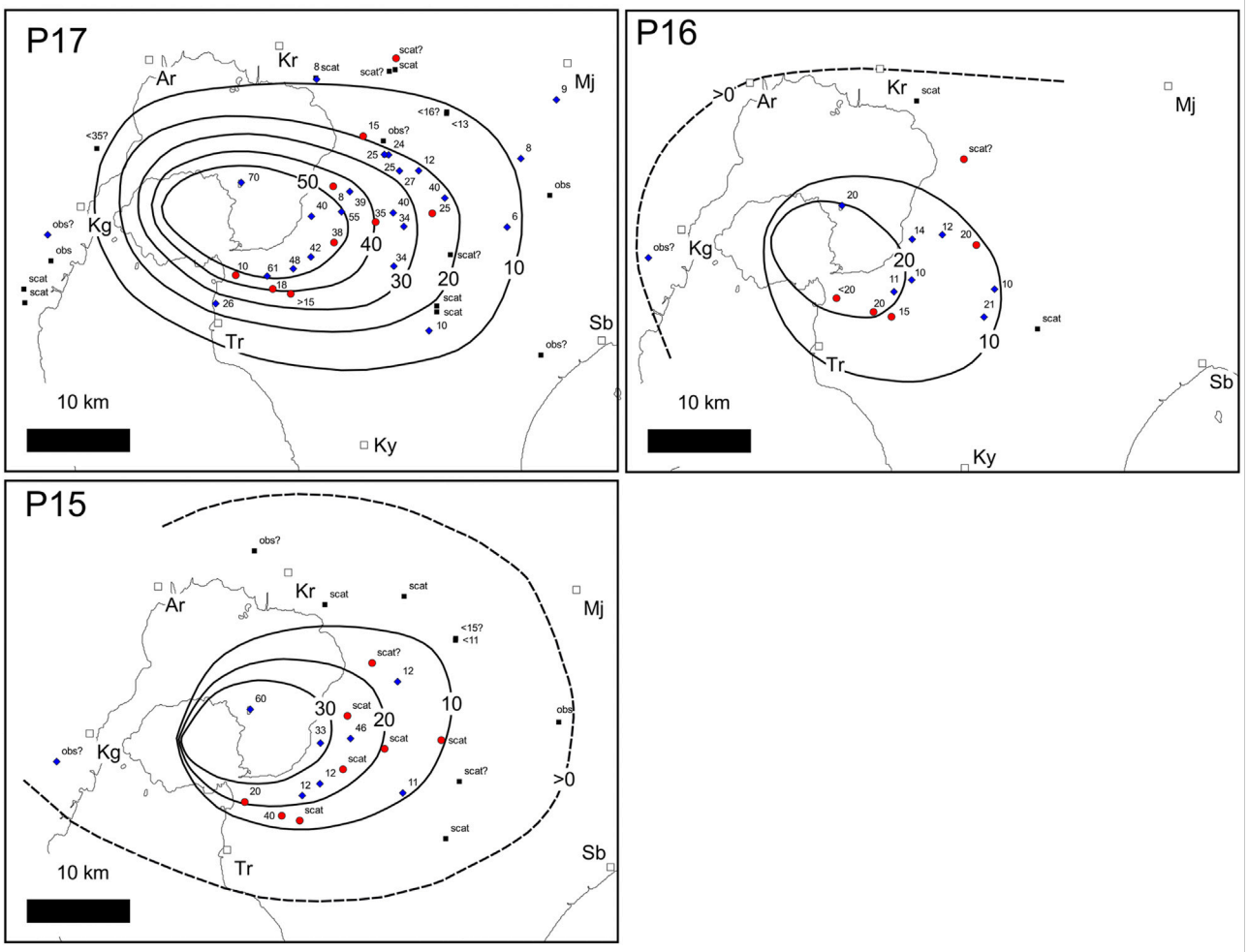

FIGURE 5
Distributions of the P17-P15 pumice fall deposits. Legend is the same in Figure 3A. The abbreviations associated with the measurement points are the following meaning; scat: outcrops where pumice lapilli was scattered in the soil, obs: localities that tephra deposits were observed without no information about lithofacies and thickness, tr: localities where tephra-derived volcanic glass and minerals were detected in soil sample analysis, although not discernible to the naked eye. Solid white squares indicate the location of major cities, and the abbreviations are the followings: Ar, Aira city; Kg, Kagoshima city; Kr, Kirishima city; Mj, Miyakonojo city; Sb, Shibushi city; Tr, Tarumizu city.

volcanic-ash bed. They often contain humus and exhibit dark color.

Kobayashi et al. (2013) summarized 17 pumice fall deposits from Sakurajima volcano, but two of the seventeen deposits (P10 and P9 tephra deposits) had been exposed only inside Sakurajima Island (Kobayashi, 1986b). The outcrop of the two tephra deposits [~30 cm and ~75 cm, respectively, extracted by the columnar section described by Kobayashi (1986a)] had already been lost. Our field survey confirmed no exposures of the two tephra outside Sakurajima Island. Although it is possible that there are other very small pumice eruptions, this study focused on 15 tephra deposits found at more than a few sites outside of Sakurajima Island.

Stratigraphy

We confirmed the stratigraphic relationships of 15 tephra deposits based on the field observations conducted on the Sakurajima edifice and surrounding region (Figure 3B).

The P17-P15 pumice fall deposits are interbedded with grayish-brownish paleosol units comprised of weathered volcanic ash particles (Figure 4A). The thickness of the soil developed between each tephra is about 20–30 cm. A thick layer of weathered volcanic ash-rich soil exists between P15 and P14 tephra deposits. The Wakamiko-derived tephra (19 ka Takano (A-Tkn) and 13 ka Shinjima (A-Sj) tephra)

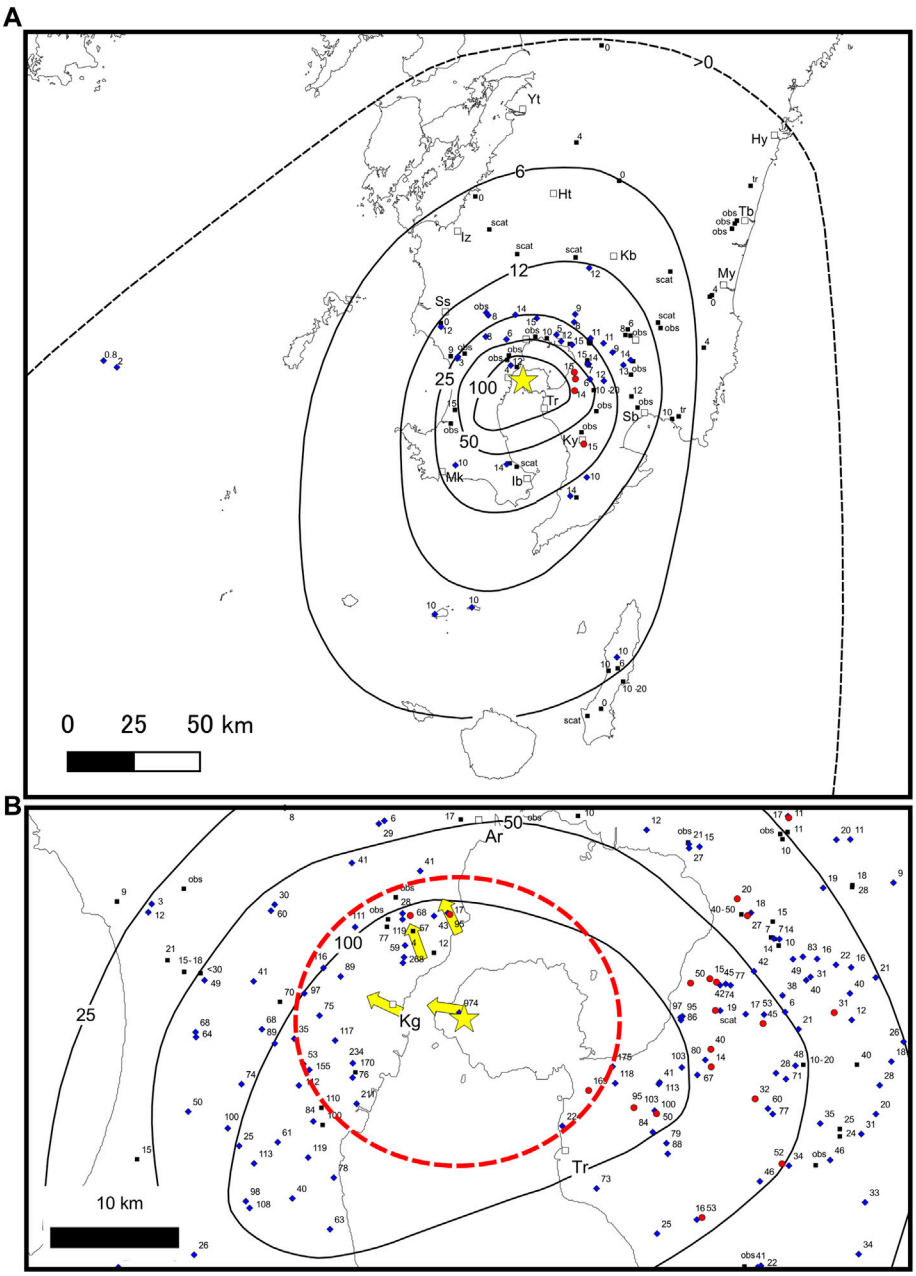

FIGURE 6
(A) Distribution of the P14 pumice fall deposit. Legend is the same in Figure 3A. The isopach contours of >12 cm are after Kobayashi et al. (2013). The points on the map show only those with ≦15 cm in thickness. The yellow arrows represent the PDC flow directions estimated from the carbonized wood contained in the P14 PDC deposits (Ishikawa et al., 1972; Kobayashi and Tameike, 1999). The yellow star in the western part of Sakurajima volcano represents the assumed vent locality of the P14 eruption (Kobayashi and Tameike, 1999). Solid white squares indicate the location of major cities, and the abbreviations are the followings: Ht, Hitoyoshi city; Hy, Hyuga city; Ib, Ibusuki city; Iz, Izumi city; Kb, Kobayashi city; Ky, Kanoya city; Mk, Makurazaki city; My, Miyazaki city; Sb, Shibushi city; Ss, Satsumasendai city; Tb, Takanabe Town; Tr, Tarumizu city; Yt, Yatsushiro city. **(B)** The distribution of the P14 tephra deposit around Sakurajima volcano. Intervals of the isopach contours are the same in Figure 6A. The dotted red line shows the assumed distributions of the P14 PDC deposit. Solid white squares indicate the location of major cities, and the abbreviations are the followings: Ar, Aira city; Kg, Kagoshima city; Tr, Tarumizu city.

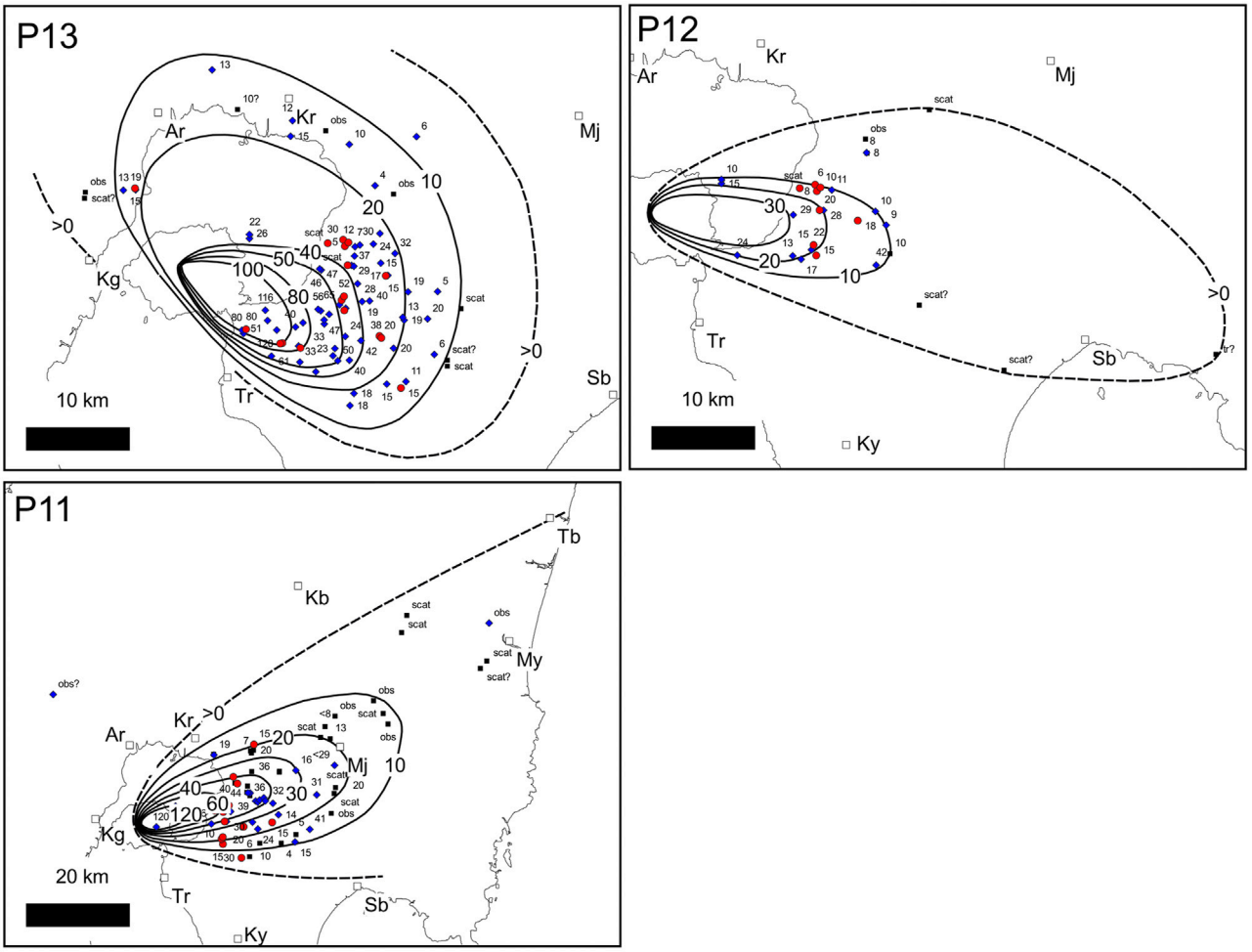

FIGURE 7
Distributions of the P13-P11 pumice fall deposits. Legend is the same in Figure 3A. Solid white squares indicate the location of major cities, and the abbreviations are the followings: Ar, Aira city; Kg, Kagoshima city; Kr, Kirishima city; Mj, Miyakonojo city; My, Miyazaki city; Sb, Shibushi city; Tr, Tarumizu city; Tb, Takanabe Town.

deposits cover the three pumice fall deposits inside the Aira caldera wall (Kobayashi, 1986b; Kano et al., 2022).

All the P14-P11 tephra deposits (Figures 4A,B) are distributed eastward from Sakurajima. Kikai-Akahoya (K-Ah) tephra is a widespread Quaternary marker bed in Japan derived from the 7.3 cal ka eruption of Kikai caldera (Machida and Arai, 1978; Okuno, 2002). The P14 and P13 tephra units are distributed northward to westward from Sakurajima below the K-Ah tephra (Figure 4F). A thick (25–60 cm) black soil is widely developed between P14 and P13 tephra deposits. In contrast, less-thick brown soils are often observed between the tephra deposits, especially at sites closer to Sakurajima (Figure 3B). The P11 tephra overlies a thin paleosol above the Yonemaru (Yn) tephra deposit, dated to be 8.1 cal ka (Moriwaki et al., 1986; Naruo, 1991; Okuno, 2002). Kobayashi and Ezaki (1996; 1997) reported that the K-Ah tephra is interbedded between P9 and P8 tephra on Sakurajima.

The stratigraphic relationships above the K-Ah tephra were confirmed in western sites (P5 tephra; Loc.1 and 2 in Figure 3; Figure 4E) and eastern-southeastern sites (P8-P7-P6; Figures 7B,D), respectively. Kobayashi and Ezaki (1996; 1997) reported that the Ikedako (Ik) tephra, erupted from the Ikeda eruption at 6.4 cal ka (Naruo and Kobayashi, 1984; Okuno, 2002), is observed between the P8 and P7 pumice fall deposits, though we could not confirm this stratigraphic relationship. Nagasako et al. (1999) reported that the Miike (Mk) tephra, which erupted from the Miike crater in the eastern part of Kirishima volcano, covered the P7 tephra. We could not confirm the stratigraphic relationship between the Miike tephra and the P6 and P5 tephra.

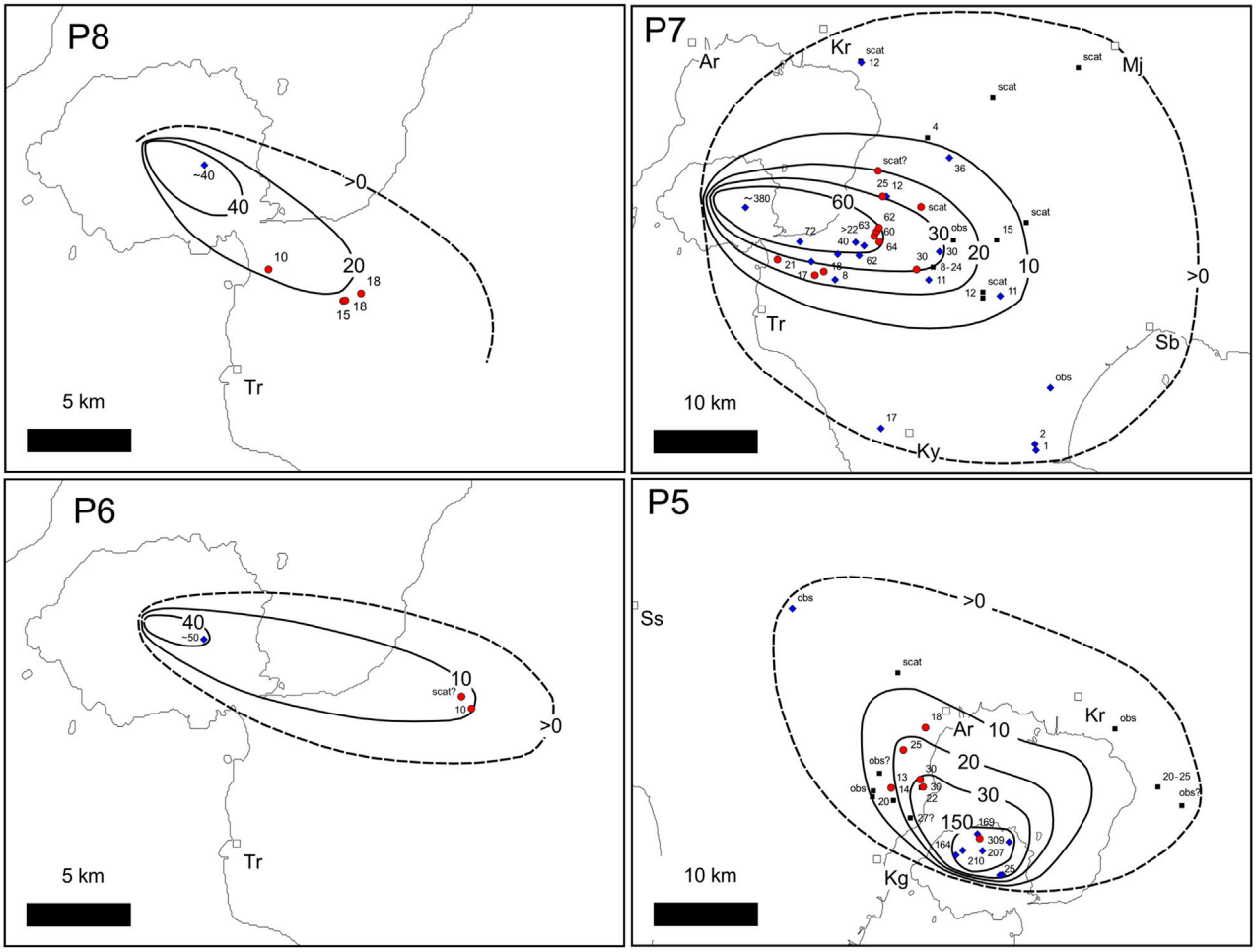

FIGURE 8
Distributions of the P8-P5 pumice fall deposits. Legend is the same in Figure 3A. The numbers of the thickness and isopach contours are described in cm. Solid white squares indicate the location of major cities, and the abbreviations are the followings: Ar, Aira city; Kg, Kagoshima city; Kr, Kirishima city; Mj, Miyakonojo city; Sb, Shibushi city; Ss, Satsumasendai city; Tr, Tarumizu city.

The P4-P1 tephra deposits lie above the P11-P5 deposits, and are intercalated with the thick volcanic sand deposit. The stratigraphic relationship between the P4 and P3 pumice fall deposits was confirmed only in the outcrop on the Sakurajima edifice (Kobayashi, 1986b). We can currently observe the relationships of the P4, P2, and P1 pumice fall deposits in the southeast (Figure 4C) and the P3-P1 pumice fall deposits in the east to northeast directions from Sakurajima.

Distribution and lithofacies

Figures 5–9 show the distribution of the pumice fall deposits of Sakurajima volcano. Vent localities of P17-P15 and P13-P5 pumice fall deposits are assumed to be around the current Kitadake summit crater for each isopach. Large images of all pumice fall deposits are reported in Supplementary Figures S1, S2. The distribution limits of the P1 (>1 cm) and P2 (>0 cm) are after Kanai (1920) and Tsukui (2011), respectively.

The P17 pumice fall deposit is widely distributed NE-SE of Sakurajima. The most distant outcrop of this tephra is 40 km NE of Sakurajima (Inoue et al., 1997). The observed maximum thickness of the P17 pumice fall deposit is 61 cm at an outcrop 10 km SE of the Kitadake summit crater (Moriwaki, 1994; Moriwaki, 2010). The direction of the central distribution axis is eastward from the Kitadake summit. Some exposures with scattered red-orange pumice, which may correspond to P17, are reported westward of Sakurajima (Kobayashi, 1989; Nishihara

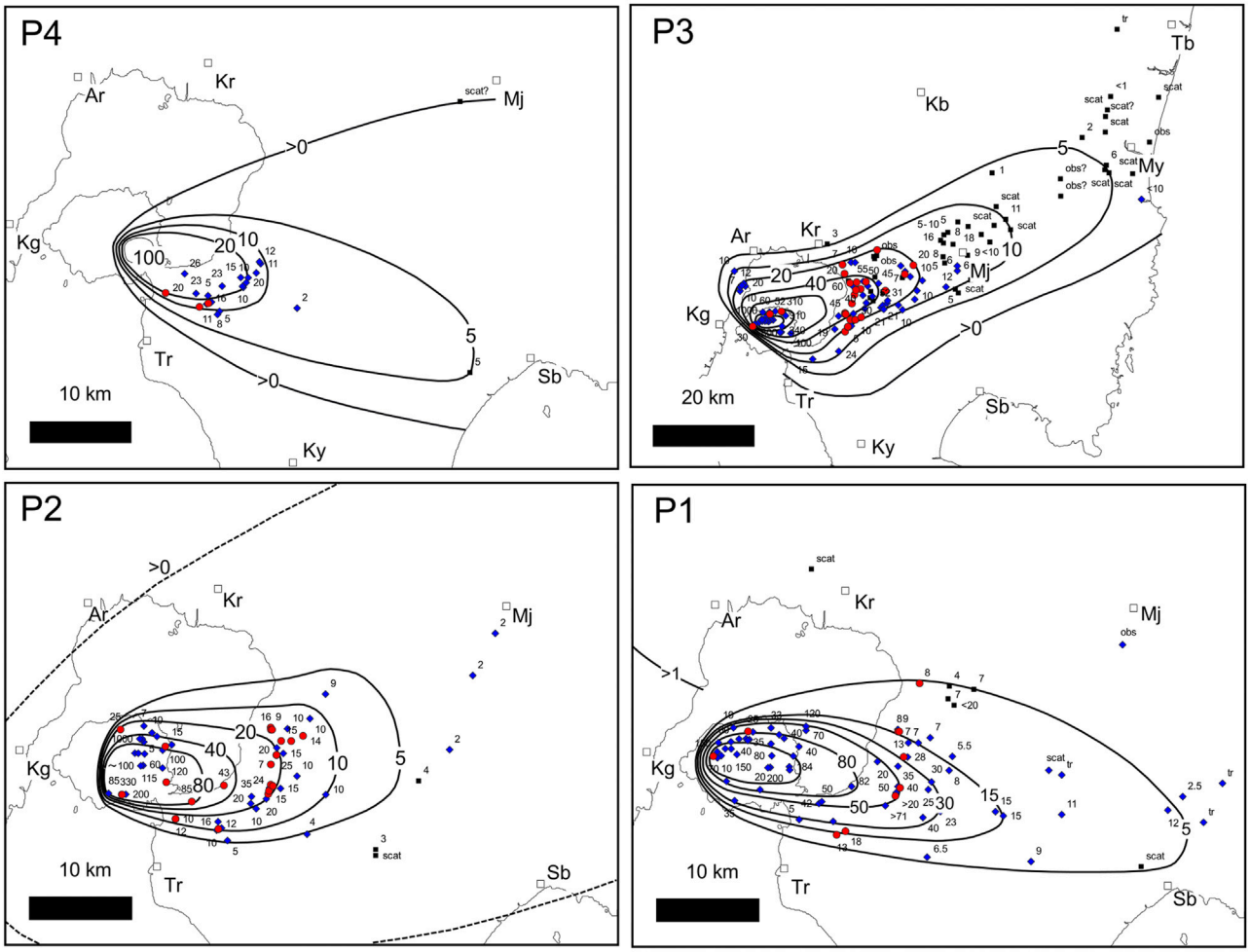

FIGURE 9
Distributions of the P4-P1 pumice fall deposits. Legend is the same in Figure 3A. The numbers of the thickness and isopach contours are described in cm. Solid white squares indicate the location of major cities, and the abbreviations are the followings: Ar, Aira city; Kg, Kagoshima city; Kr, Kirishima city; Mj, Miyakonojo city; My, Miyazaki city; Sb, Shibushi city; Tr, Tarumizu city; Tb, Takanabe Town.

et al., 2022, and reference therein). The P17 pumice fall deposit has three sub-units made up of reddish pumice lapilli, black scoria lapilli, yellow-orange ash, and blue-gray igneous lithic fragments. At Loc. 6 in Figure 3, the P17 with two sub-units is observed; the lower unit is well-sorted and comprises ash and lapilli of pumice, scoria, and igneous lithic fragments, and the upper one consists of ash with a scattering of pumice and igneous lithic lapilli. An inversely graded pumice-lapilli bearing tephra deposit, comprising weathered pumice clasts and lithic fragments from the P17 eruption, was described from the borehole core at Shinjima, off the northeastern coast of Sakurajima (Kano et al., 2022).

The P16 and P15 pumice fall deposits with thicknesses >10 cm are distributed within ~20 km and ~25 km from the Kitadake summit, respectively (Figure 5). The two tephra units can also be recognized westward from Sakurajima (Kobayashi, 1989). The P16 and P15 tephra deposits were described in the Shinjima borehole core (Kano et al., 2022). The P16 pumice fall deposit at Loc. 9 consists of lapilli of yellow-orange pumice and a small amount of gray igneous lithic fragments, whereas the P15 one showing normal grading consists of red-orange pumice lapilli, orange ash, and blue-gray igneous lithic fragments. Some exposures of the P15 pumice fall deposits contain accretionary lapilli (Moriwaki, 1994).

The P14 tephra is distributed in all directions from Sakurajima (Moriwaki, 1992; Kobayashi and Tameike, 1999). The P14 tephra has the largest distribution area among the pumice fall deposits of Sakurajima (Figure 6). The P14 tephra mainly consists of pumiceous lapilli and lithic fragments as air fall and PDC deposits (Moriwaki, 1992; Kobayashi and Tameike, 1999). The farthest distributions reached by the P14 tephra are so far ~90 km to the north and ~2,350 km to the south

(Paleoenvironment Research Institute, 2002; Sun et al., 2021). The PDC deposit of the P14 tephra is mainly distributed within 10 km to the west of Sakurajima (Moriwaki, 1992; Kobayashi and Tameike, 1999) and was also described at Loc. 9, to the east from Sakurajima. The maximum thickness of the PDC deposit is 9.74 m as observed in borehole core samples on Sakurajima (Yamamoto et al., 2013). Kobayashi and Tameike (1999) assumed that the vent of the P14 tephra was located in the western part of Sakurajima, shown by the yellow star in Figure 6, based on the thickness flow directions of the PDC deposits estimated from the carbonized wood contained in the P14 PDC deposits (Ishikawa et al., 1972; Kobayashi and Tameike, 1999). At Loc. 2, the P14 tephra deposit has several sub-units made up of lapilli to volcanic rock of orange pumice, black and red igneous lithics, and a small amount of white-colored altered rock (Figure 4E).

The P13 pumice fall deposit is widely distributed around Sakurajima, and is especially thick to the SE. The P13 tephra consists of three sub-units from the base: P13a, P13b, and P13c (Okuno et al., 1999; Kobayashi and Tameike, 2002). The P13a and 13b units are mainly distributed SE-E of Sakurajima, whereas the P13c unit is widely distributed around Sakurajima (Okuno et al., 1999; Kobayashi and Tameike, 2002). At Loc. 9, all three units can be observed. The P13a and P13b units are composed of orange and gray pumice clasts (lapilli-volcanic rock) and black igneous lithic fragments are distributed mainly SE of Sakurajima. The P13a and P13b pumice lapilli show normal and reverse grading, respectively. The P13c unit consists of finer pumice lapilli and igneous lithic fragments.

The P12 pumice fall deposit is distributed E of the Sakurajima. The distribution of the P12 tephra is very elongated in the major axis direction, but its north-south spread in the orthogonal direction is narrow. The P12 pumice fall deposit consists of well-sorted pumice lapilli and free crystals with few black igneous lithic fragments. The maximum thickness of P12 is described as 29 cm at 13 km E from the Kitadake summit (Moriwaki, 1994).

The P11 pumice fall deposit is widely distributed NE of Sakurajima, showing an elongated distribution pattern toward the NE direction. The most distant point described is ~90 km northeast of Sakurajima (Kuwahata et al., 2021; Nishihara et al., 2022, and reference therein). The maximum thickness of the tephra described outside the Sakurajima edifice is 130 cm at an outcrop 7 km east-northeast of the Kitadake summit crater (Moriwaki et al., 2017). The thickness of the P11 pumice fall deposit was described to be ~4.5 m at an outcrop on Sakurajima, which is located 2.5 km east from the Kitadake summit (Kobayashi, 1986b). The direction of the main distribution axis is northeastward from the Kitadake summit. At Loc. 5, the P11 pumice fall deposit with three sub-units is made up mainly of, from the bottom, (1) lapilli of orange pumice and small amounts of black igneous lithics, (2) ash and lapilli of pumice, crystals, and lithics, and (3) lapilli to blocks of pumice and lithics.

The P8 pumice fall deposit is distributed within 13 km SE of Sakurajima. P8 consists of white-orange pumice lapilli covered with white-colored ash. The maximum thickness values of the P8 tephra in exposures on and outside the Sakurajima edifice are ~40 cm (Kobayashi, 1986b) and 18 cm in Loc.8–1, respectively.

The P7 pumice fall deposit is distributed E of Sakurajima. The most distant point described is 40 km SE of Sakurajima (Nagasako et al., 1999). The P7 tephra deposit consists of pumice lapilli with small amounts of lithic fragments. Some depositional units comprising pumice lapilli and ash are recognized nearby Sakurajima. The thick pumice fall deposit of >60 cm is exposed within <15 km from the Kitadake summit. The proximal thickness at the outcrop on Sakurajima was described as ~3.8 m (Kobayashi, 1986b). At Loc. 7, the P7 pumice fall deposit with three sub-units is exposed, composed of ash to lapilli of orange-gray pumice and a small amount of igneous lithic fragment. The lowest and middle sub-units of 22 cm and ~10 cm thick show weakly reverse and normal grading, respectively.

The P6 pumice fall deposit, mainly comprising orange pumice lapilli, is distributed within 16 km E-SE of Sakurajima. The thickness of the P6 deposits inside and outside Sakurajima is 48 cm (Kobayashi, 1986b) and 10 cm, respectively. The P6 pumice fall deposit at Loc. 6 consists of ash to fine lapilli of yellow pumice and small amounts of gray-black igneous lithic fragments and shows normal grading.

The P5 tephra is distributed NW-NE of Sakurajima, and the most distant point described is 30 km NW from Sakurajima (Hayashida et al., 2022). The P5 eruption discharged a PDC deposit (Take PDC deposit; Kobayashi, 1986b; Hiramine et al., 2015) associated with the P5 pumice fall deposit. The Take PDC deposit is distributed on the northern flank of the Kitadake edifice (Kobayashi, 1986b; Hiramine et al., 2015). The P5 pumice fall deposit, comprising orange pumice lapilli, is the only tephra with its main distribution axis toward the northwest of Sakurajima. The direction of the main distribution axis is NW from the Kitadake summit. The maximum thickness of the tephra described outside Sakurajima is 30 cm at an outcrop 10 km NW from the Kitadake summit crater. Kobayashi and Ezaki (1996) reported that the P5 tephra composed of lithified fine volcanic ash is distributed northward from Sakurajima.

The P4 pumice fall deposit is distributed SE of Sakurajima. The most distant identified point is 39 km from Nabeyama, which is the tuff cone vent site of the P4 eruption (Kobayashi, 1982; Naruo and Geshi, 2020). The maximum thickness of the tephra observed outside Sakurajima is 26 cm at an outcrop 8 km ESE of the Minamidake summit (Moriwaki, 1994). The direction of the main distribution axis is southeastward. The P4 pumice fall deposit is composed of yellow pumice lapilli and white ash. Three depositional units of the P4 pumice fall deposit are observed near Sakurajima (e.g., Loc. 9).

The P3 pumice fall deposit is widely distributed NE of Sakurajima, showing an elongated distribution pattern toward the NE direction. The most distant point described is ~90 km northeast of Sakurajima (Ikuta et al., 2016; Nishihara et al., 2022, and reference therein). The observed maximum thickness of the tephra is 10 m at an outcrop 2.5 km SE of the Minamidake summit crater (Iwamatsu and Kobayashi, 1984). The direction of the main distribution axis is northeastward from the Minamidake summit. The P3 tephra consists of pumice fall deposits and interbedded layers of PDC deposits on the northern slope of Kitadake (Kobayashi, 1986b). Outside of Sakurajima, the P3 pumice fall deposit mainly comprises lapilli of pumice and igneous rock.

The P2 pumice fall deposit is widely distributed E of Sakurajima, and the most distant point described is 40 km east of Sakurajima (Kobayashi and Ezaki, 1996). The maximum thickness of the tephra is 10 m (Iwamatsu and Kobayashi, 1984) at an outcrop near the An-ei crater (2.4 km east of the Minamidake summit crater). The direction of the main distribution axis is eastward from the Minamidake summit. The P2 pumice fall deposits at Loc. 7-9 consists of fine lapilli of white pumice and small amounts of igneous lithic fragments.

The P1 pumice fall deposit is distributed east of Sakurajima, showing an elongated distribution pattern from the 1914 eruption fissures toward the E direction. The most distant point described is ~50 km east of Sakurajima (Todde et al., 2017). The observed maximum thickness of the tephra is 5 m at an outcrop 2.7 km west of the Minamidake summit crater (Iwamatsu and Kobayashi, 1984). The direction of the main distribution axis is eastward from the Minamidake summit. Todde et al. (2017) reported that the P1 pumice fall deposits could be subdivided into three lapilli-bearing units (Units T1, T2, and T3, which correspond to the subPlinian phase) and one ash-bearing unit (Unit T4, which corresponds to the final ash venting).

Radiocarbon ages

In this study, we measured the ^{14}C ages of three charcoal samples associated with P5 and P7 tephra deposits because the previously reported ages of these units are inconsistent with their stratigraphic relationships (Okuno, 2002; Kobayashi et al., 2013). Table 2 lists the results of AMS radiocarbon dating in this study.

The charcoal sample (211115E-C03) collected from the base of the P5 tephra yielded a ^{14}C age of 4,210 years BP, corresponding to 4.8 cal ka BP. Another charcoal sample (211117A-C01) collected from the paleosol below the P5 pumice fall deposit yielded a ^{14}C age of 4,640 years BP, corresponding to 5.4 cal ka BP. The charcoal sample (211114C-C02) in the paleosol below the P7 pumice fall deposit yielded a ^{14}C age of 5,100 years BP, corresponding to 5.8 cal ka BP.

Estimation of the age of the P7-P5 tephras

Two ^{14}C ages associated with P5 tephra obtained by this study are consistent with their stratigraphic relationship. The ^{14}C age obtained from the charcoal sample (211117A-C01) collected from the paleosol ~5 cm below the P5 pumice fall deposit is ~0.6 kyr older than that of the charcoal sample (211115E-C03) collected from the base of the P5 tephra. This 0.6 kyr time gap between two ^{14}C ages is suggested to represent the forming of a 5 cm-thick soil between the charcoal sample of 211117A-C01 and P5 tephra. The K-Ah ashfall deposit erupted at 7.3 cal ka (Okuno, 2002) provides a time control of the growth of paleosol. At Loc. 2, the thickness of paleosol between the sampling level of 211117A-C01 (5.4 cal ka; this study) and K-Ah is ~30 cm (Figure 3B). This gives a formation rate of soil ~16 cm/1,000 years. Based on this rate, the age of P5 at ~5 cm above the sampling level of 211117A-C01 (5.4 cal ka) can be estimated as ~5.1 cal ka. This estimated age is consistent with the ^{14}C age obtained from the base of P5 tephra of 211115E-C03 (4.8 cal ka). Thus, we estimated the age of P5 tephra as 4.8 cal ka. This age is younger than the age (5.6 cal ka) reported by Okuno (2002).

The age of P7 presented by this study (5.8 cal ka BP) is older than the age (5.0 cal ka) proposed by Okuno (2002), though our ^{14}C age may be slightly older than the eruption age of P7, as our ^{14}C age is obtained from the charcoal fragments in the paleosol below P7 tephra. The previous estimate of the age of P7 is close to the age of the P5 tephra deposit proposed by this study and is inconsistent with the development of 40 cm-thick paleosol between P7 and P5 at the eastern flank of Sakurajima (Kobayashi, 1986b), suggesting a time gap between deposition of the two tephra units.

Our new dating results of the P7 and P5 eruption ages also necessitate an additional reexamination of the P6 eruption age. In the outcrop at the eastern base of Sakurajima (Kobayashi, 1986b), where all tephras from P7 to P5 are exposed, the thickness of soil layers between each tephra is almost the same, suggesting that the P6 tephra was discharged ~5.3 cal ka. The previous study's eruption age of the P6 tephra is assumed to be 3.8 cal ka BP, based on the carbon in the soil below the P6 tephra away from the edifice (Okuno et al., 1997; Okuno, 2002). However, this value is too young. In ^{14}C dating for soil samples, the sample with a low C/N ratio (<10) tends to provide a young age (e.g., Okuno et al., 1997). The C/N ratio of soil sample for determining the P6 eruption age is 8.2 (Okuno et al., 1997; Okuno, 2002), suggesting that it may have provided an inaccurately young ^{14}C age. Thus, we conclude that the eruption age of the P6 tephra (5.3 cal ka BP) inferred from the soil-formation rate is appropriate.

Evaluation of the tephra volume

Tephra volume recalculations were examined using the new isopach maps redrawn by our field observations and

TABLE 2 Results of the AMS ^{14}C dating.

Tephra	Locality	sample	Lab. ID.	Sample ID	Age (year, ±1σ)	IntCal20 age (cal. kyr)
P7	Loc. 8–1	charcoal	IAAA-211296	211114C-C02	5,100 ± 30	5.8
P5	Loc. 3	charcoal	IAAA-211297	211115E-C03	4,210 ± 20	4.7–4.8
P5	Loc. 2	charcoal	IAAA-211298	211117A-C01	4,640 ± 20	5.4

compiled data. Our volume estimation of each tephra is minimum because the current thickness of tephra deposits is likely smaller than the original one. Calculations of areas surrounded by the given isopach were conducted by QGIS software. The calculations were performed by methods of exponential fitting (Pyle, 1989; Fierstein and Nathenson, 1992), the power-law fitting (Bonadonna and Houghton, 2005), and the Weibull fitting methods (Bonadonna and Costa, 2012). A conventional calculation method for tephra volumes proposed by Hayakawa (1985) was also conducted. The explorations for the Weibull parameters were performed using AshCalc software (ver. 1.2; Daggitt et al., 2014). The calculation results are summarized in Table 3, and detailed parameters for the calculations are listed in Supplementary Table S4.

The exponential and power-law fitting calculations give similar results. The estimations by the method of Hayakawa (1985) are systematically larger than the results by the other three methods. This may be because the empirical rule used in Hayakawa (1985) was derived from large-scale Plinian eruptions and does not hold for small-scale pumice eruptions of Sakurajima, which are the subject of this study.

Another problem with the calculations is that some results based on the Weibull methods are larger than results obtained with the other two methods (for the results of the P2, P4, P5, and P8 tephras). In addition, the Weibull parameter of λ for the P14 tephra is too large (Supplementary Table S4). The cause of this is unclear, but the calculations for these tephra deposits may not be working well because the isostatic thickness lines created based on the existing layer thicknesses are partially different from the original ones. Bonadonna et al. (2015) suggested that an average volume of the three methods is good for the estimated tephra volume. However, the difference in the volume of tephras by more than an order of magnitude cannot be ignored. Thus, we consider the average values of the three methods as the best values of the tephras without any contour problems, and those of the two methods except for the problem method for the others (Table 3).

The estimated volume of each tephra is smaller than the previous estimation by Kobayashi et al. (2013), mainly due to the difference in calculation methods (Table 3), but we obtained nearly identical estimates for the P1 pumice fall deposits reported by Todde et al. (2017), which were calculated using a similar methodology to that in this paper. Our estimated volume of P14, the largest tephra of Sakurajima, as 11 km^3, is also in agreement with the estimate by Kobayashi and Tameike (1999) because we re-evaluated the far-field distribution of the tephra (e.g., Sun et al., 2021). Three major pumice fall deposits (P13, P11, and P3) are evaluated as ~0.5 km^3 in volume. The volumes of the pumice fall deposits P8 and P6, only identified in and around Sakurajima, were evaluated to be less than 0.04 km^3 in each case. The values of the volcanic explosive index (VEI; Newhall and Self, 1982) of each eruption are shown in Table 4. The total volumes of the pumice fall deposits of Stage 1, Stage 2, and Stage 3 are estimated as 0.76, 12.7, and 1.1 km^3, respectively.

Estimated tephra volumes were converted to dense rock equivalent (DRE) volumes. The measurement of bulk density of the pumice clast comprising the P1 pumice fall deposit indicates that the representative bulk density of the P1 pumice clast is 700 kg/m^3 but shows a range of 300–1,700 kg/m^3 (Nakamura, 2006). In this paper, 1,000 kg/m^3 is used for the density of the pumice fall deposit for the DRE calculation. The value of 1,200 kg/m^3 is used for the density of the pyroclastic density current deposit (Umeda et al., 2013). The calculation results are summarized in Table 4 (the density of lava is assumed to be 2,500 kg/m^3).

We also calculated the eruption magnitude of each eruption (Hayakawa, 1993; Pyle, 1995) that occurred at Sakurajima. The calculations required the volume of magma discharged by all phases of each eruption (e.g., lava and PDC deposits. The volume of the P5 PDC deposit is 0.03 km^3 (Hiramine et al., 2015). The volume of the P14 PDC deposit is assumed to be 0.25 km^3, which is calculated from the assumption that the PDC deposit with 0.8 m-thickness covers the inferred distribution area described in Figure 6B. The calculation results are summarized in Table 4. Based on the duration and magma volume erupted as tephras, the average magma discharge rates in each stage are calculated as follows; 0.05 km^3/kyr of Stage 1 (30–24 ka), 0.6 km^3/kyr of Stage 2 (12.8–4.8 ka), and 0.1 km^3/kyr of Stage 3 (4.5 ka–present).

TABLE 3 Results of the tephra volume calculations for Sakurajima volcano.

Tephra	Volume (km^3)					
	exponential	power-law	Weibull	12.2*TS	accepted value	Kobayashi et al. (2013)
P1	0.25	0.28	0.31	0.59	0.28	0.5
P2	0.19	0.26	3.7	0.35	0.22	0.3
P3	0.52	0.49	0.58	0.92	0.53	0.8
P4	0.098	0.067	0.58	0.14	0.082	0.1
P5	0.18	0.18	3.0	0.35	0.18	0.4
P6	0.020	0.024	0.054	0.041	0.022	<0.1
P7	0.22	0.23	0.40	0.57	0.29	0.7
P8	0.034	0.041	0.708	0.077	0.037	<0.1
P11	0.47	0.46	0.56	0.97	0.50	1
P12	0.069	0.088	0.065	0.21	0.074	<0.1
P13	0.39	0.40	0.55	0.87	0.45	1.3
P14	7.4	15	21	13	11.1	11
P15	0.17	0.16	0.13	0.51	0.15	0.2
P16	0.15	0.12	0.41	0.37	0.23	0.3
P17	0.39	0.39	0.37	1.2	0.38	1.1

Discussion

Variation in eruptive rate during Stage 2

Our new estimation of the volume of magma reveals that Stage 2 produced 5.2 km^3 DRE of magma as tephra. The volume of lavas should also be counted for the magma discharge rate in addition to the volume of tephra. We surmise that the formation of most of the Kitadake edifice commenced after the P14 eruption because the phreatomagmatic characteristics of P14 tephra (Moriwaki, 1992) suggest that the elevation of the crater of Kitadake was near sea-level at the time of the P14 eruption, meaning that no high volcanic edifice was present at the beginning of Stage 2. We also surmise that most of the Kitadake edifice was built during the early Stage 2, based on the ages of lava (10.5–9.5 ka; Miki et al., 2003; Uto et al., 2005) distributed at the surface of the northern slope of Kitadake, though a small amount of the younger PDC products discharged by the P5 eruption also cover the northern Kitadake edifice (Kobayashi, 1986b; Hiramine et al., 2015). The total volume of the Kitadake edifice is estimated to be about 12.5 km^3 (see Supplementary Material for calculation method).

For the evaluation of the total volume of erupted magmas in Stage 2, the volume of the pumice fall deposits within the Kitadake edifice should be removed from the volume of the edifice, because this value could contain the pumice fallout deposited near the vent, and maybe a duplicate count of the volume of the pumice fallout. The total volume of the pumice fall deposits distributed within the Kitadake edifice is estimated to be 0.95 km^3, inferred from calculations with the power-law fitting methods, which is 6.5% of the total volume of the pumice-fall deposits since Stage 2 (detailed method is described in the Supplementary Material for calculation method). Except for the pumice fall deposits, the Kitadake edifice consists of lava, agglutinate, and PDC deposits. Assuming a density of 1,900 kg/m^3 (Umeda et al., 2013) for the edifice, the volume of magma for the building of the Kitadake edifice is 8.8 km^3 DRE. Thus, the total volume of erupted magma during Stage 2 is estimated as ~14 km^3.

The estimated volume of each pumice fall deposit and the edifice of Stage 2 shows a prominent magma discharge rate at the beginning of the stage (2.9 km^3/kyr), followed by a marked decrease in the magma discharge rate (0.07 km^3/kyr; Figure 10). The P14 eruption (12.8 cal ka) at the beginning of Stage 2 discharged 4.6 km^3 DRE of magmas, corresponding to 33% of the total erupted magmas during Stage 2. The effusion of voluminous lava followed the P14 eruption flows comprising the Kitadake edifice (8.8 km^3 DRE), which corresponds to 63% of the total magma discharged during Stage 2. The value of 8.8 km^3 DRE also contains the lateral vent lava (Harutayama lava), which erupted at 9 ka or 7 ka (Miki et al., 2000; Uto et al., 2005). We presume that the eruption age of the Harutayama lava occurred at 9 ka since the Gongenyama lava at the eastern base, which has a similar chemical composition and is considered to have erupted around the same time, is covered with the 8.0 ka P11 pumice fall deposit (Miki et al., 2003; Kobayashi et al., 2013; Takahashi et al., 2013). Based on this presumption, the

8.8 km^3 magma had been discharged before the P11 eruption. The volume of magma discharged by the three large eruptions (P13-P11 eruptions) is 0.41 km^3. Thus, more than 98% of the magma in Stage 2 erupted during ~4,800 years from the beginning of the stage.

These observations argue that a high discharge rate occurred in early Stage 2, followed by a decline in activity. As discussed above, the volcanic activities at 13–8 ka are characterized by more explosive eruptions and voluminous lava effusions comprising the Kitadake edifice. The explosive activities at ~1 kyr-intervals continued until 8.0 ka. After the P11 eruption, pumice-bearing eruptions occurred more frequently at intervals of 0.2–1.0 kyr. These observations showed that the eruption style likely changed after the P11 eruption (8.0 cal ka).

The fine volcanic ash deposits that exist above the P11 pumice fall deposit indicate that ash-producing activity occurred after the P11 eruption. Thick yellowish-brown aerial deposits were observed between the P11 and P7 or P5 pumice fall deposits in eastern and western outcrops on Sakurajima. Kobayashi (1986a) describes a thick ashy soil above P11 in the outcrop at the Kitadake flank. These ash-producing activities at the end of Stage 2 suggest a change in activity from explosive pumice eruptions with higher magma discharge rate to the ash-producing Vulcanian eruptions with a decrease in magma discharge rate during Stage 2. Corresponding to these changes in eruption activities, we propose that Stage 2 can be subdivided into two sub-stages of Stage 2a (12.8–8.0 ka) and 2b (8.0–4.5 ka).

The difference in eruption styles between Stage 2 and Stage 3

The heightened level of volcanic activity during Stage 2a shifted to moderate-sized and frequent eruptions in Stage 2b, which is in contrast to the evolution of the eruption styles from Stage 3a (4.5–1.6 ka) to Stage 3b (AD 764–present; ~1.3kyr). The activities of Minamidake started with repeated effusive and ash-producing Vulcanian eruptions in Stage 3a and then shifted to pumice eruptions with lava effusions in the younger Minamidake stage. The relatively low magma discharge rate in Stage 3a (1.1 km^3/kyr) also shifted to a higher one in Stage 3b (4.0 km^3/kyr). The high magma discharge rate of Stage 3b has been noted in previous studies (e.g., Kobayashi et al., 2013; Yamamoto et al., 2018), and the reexamination of the tephra volume conducted in this study confirms this trend. In addition, elucidating the activity transition in Stage 2 can clarify the difference from the activity transition in Stage 3.

The four historical pumice-producing eruptions in Stage 3b discharged pumice clasts and lavas (Kobayashi, 1982). The ratios of volume of magma erupted as lava/pyroclastic products were

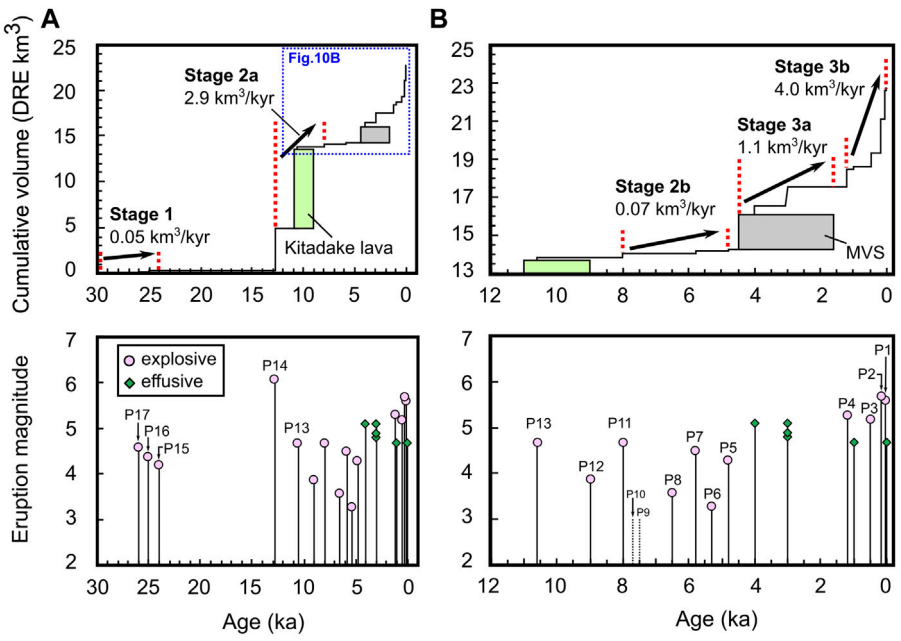

FIGURE 10
Temporal variations of the magma discharge rate of Sakurajima volcano. The upper panels of Figures 10A,B show a diagram of cumulative discharged magma volume with time. Squares describe the Kitadake lava (green) and the Minamidake Volcanic Sand (MVS; gray) with estimated cumulative eruption durations and volumes. The lower panels show the eruption magnitude of each eruption (see Table 4). **(A)** shows the entire activity of Sakurajima, and **(B)** shows the activities within the last 12,000 years. Note that the vertical axis values of the upper image in Figures 10A,B are not the same.

TABLE 4 Summary of the eruptive history of Sakurajima volcano. Volume of lavas (Ishihara et al., 1981; Miki and Kobayashi, 2016) includes both subaerial and submarine distributions.

Eruption	Age	Volume (km^3)				VEI	km^3 DRE					Magnitude
		fallout	PDC	lava	edifice		fallout	PDC	lava	edifice	total	
Stage 3b (Younger Minamidake stage)												
Showa	AD 1946			0.18[a]					0.18		0.18	4.7
P1 (Taisho)	AD 1914–15	0.28		1.34[a]		4	0.11		1.34		1.5	5.6
P2 (An-ei)	AD 1779–82	0.22		1.7[a]		4	0.090		1.7		1.8	5.7
P3 (Bunmei)	AD 1471–76	0.53		0.49[a]		4	0.21		0.49		0.70	5.2
Ohira	AD 950[b,c]			0.2[d]					0.2		0.20	4.7
P4 (Tenpyo-hoji)	AD 764–766	0.082		0.84[d]		3	0.033		0.84		0.87	5.3
Stage 3a (Older Minamidake stage)												
Kurokamigawa	~3 ka[d]			0.23[d]					0.23		0.23	4.8
Arimura	~3 ka[d]			0.47[d]					0.47		0.47	5.1
Kannonzaki	~3 ka[d]			0.32[d]					0.32		0.32	4.9
Miyamoto	~4 ka[e]			0.46[d]					0.46		0.46	5.1
MVS	4.5–1.6 cal ka[f]	3.5[d]					1.8[d]				1.8	
Stage 2b (late Younger Kitadake stage)												
P5	4.8 cal ka	0.18	0.03[g]			4	0.071	0.014			0.086	4.3
P6	5.3 cal ka	0.022				3	0.0087				0.0087	3.3
P7	5.8 cal ka	0.29				4	0.11				0.11	4.4
P8	6.5 cal ka[f]	0.037				3	0.015				0.015	3.6
P9	7.5 cal ka[f]	unknown										
P10	7.7 cal ka[f]	unknown										
Stage 2a (early Younger Kitadake stage)												
P11	8.0 cal ka[f]	0.50				4	0.20				0.20	4.7
P12	9.0 cal ka[f]	0.074				3	0.030				0.030	3.9
P13	10.6 cal ka[f]	0.45				4	0.18				0.18	4.7
Kitadake edifice	11–9 ka				11.6					8.8	8.8	
P14 (Satsuma)	12.8 cal ka[f]	11.1	0.25			6	4.44	0.12			4.6	6.1
Stage 1 (Older Kitadake stage)												
P15	24 cal ka[f]	0.15				4	0.061				0.061	4.2
P16	25 cal ka[f]	0.23				4	0.092				0.092	4.4
P17	26 cal ka[f]	0.38				4	0.15				0.15	4.6

[a]Ishihara et al. (1981).
[b]Kobayashi et al. (2009).
[c]Miki et al. (2012).
[d]Miki and Kobayashi (2016).
[e]Miki (1999).
[f]Okuno (2002).
[g]Hiramine et al. (2015).

calculated to be 12 for P1, 19 for P2, 2.3 for P3, and 25 for P4 (Table 4). Except for the P3 eruption, most of the magma that erupted in each eruption erupted as lava. If the explosive eruptions in Stage 2 erupted lavas at the same lava/pumice rate as P3, the estimated volume of lava erupted would be >11 km^3. This value is larger than the DRE volume of the Kitadake edifice, indicating that this situation is not suitable. Thus, even if explosive eruptions during Stage 2 produced lava, the ratio is smaller than that of the historical eruptions themselves, suggesting that the eruptions in Stage 2 were more explosive than those in Stage 3b.

Availability of tephra deposits for unraveling the volcanic history

Geological analysis of the sequence, lithofacies, and volume of widely-distributed pumice fall deposits is an important method for the reconstruction of the eruption history of their source volcano. The pumice fall deposits analyzed in this study are the products of sub-Plinian to Plinian explosive eruptions and are typical "master events" (Szakács et al., 2010) of Sakurajima volcano.

However, the master event-based analysis of the volcanic activities using pumice fall deposits in the distal area has several problems that should be addressed. The first one is the "representativeness" of these master events for volcanic activity. Because the sum of the estimated volume of 15 pumice fall deposits of Sakurajima occupies only ~6.5% of the stratovolcano edifice of Sakurajima, which is predominantly composed of lava flows and near-vent deposits. This suggests that the activity history obtained from pumice fall deposits may not cover most of the magmatic eruption activity. Observations of some recent pumice eruptions of Sakurajima show that the pumice eruptions of Sakurajima accompanied effusive activity with a much larger volume of magma discharge (Ishihara et al., 1981; Miki and Kobayashi, 2016). For example, in the P4 and P3 eruptions that show similar eruption magnitudes (5.3 and 5.2, respectively), the ratio between magma erupted during the effusive phase and magma erupted during the pumice phase is 25 and 2.3. This result indicates the utility of examining the relationship between explosive activity that produces widely-distributed pumice fall deposits and effusive activity that contributes to the building of volcanic edifices.

The second point is the evaluation of apparent repose periods in volcanic activity. Though repose is an important indicator of the time sequence of volcanic activity (Szakács et al., 2010), it is difficult to identify whether periods of no preservation for pumice fall deposits reflect repose or an active period of lower intensity explosive or effusive activities. The development of unconformities may also be an indicator of dormant periods. However, the relationship between the presence of unconformities in the pile of tephra deposits in each outcrop and repose periods of volcanic activity is unclear at Sakurajima since active and heterogeneous erosional activity on land in areas with topographic relief and significant precipitation promotes the development of localized unconformities. Tracing aerial deposits interbedding the pumice fall deposits (analysis of component, weathering, pollen, and humic material) from proximal to distal areas of a volcano may offer clues for solving this problem, in addition to precise dating of each pumice fall deposit.

Despite these unresolved issues, the stratigraphic analysis of pumice fall deposits distributed over a wide area is a powerful tool for deciphering the growth history of complex stratovolcanoes. The case study of Sakurajima presented here demonstrates that the distribution and stratigraphy of pumice layers based on tight field surveys with intense dating should be attempted at various volcanoes to promote the advancement of the method.

Conclusions

We reexamined the distribution, volume, and age of the pumice fall deposits and clarified the Sakurajima volcano's long-term temporal variations of volcanic activities as follows:

1. The eruption history of Sakurajima volcano can be broadly divided into three stages; Stage 1, Stage 2, and Stage 3. Reexamination of the distribution and eruptive volume of the pumice-bearing eruptions reveal that the total amount of magma erupted as the pumice fallout is 5.8 km^3 (14.5 km^3 tephra), which is smaller than the previous estimation (18.2 km^3 in volume; Kobayashi et al., 2013).
2. The eruption age of the P7 and P5 eruptions is estimated at 5.8 and 4.8 cal ka, respectively, based on new ^{14}C data. The age of the P6 eruption is assumed at 5.3 cal ka. These new dating results indicate that the pumice-bearing eruptions occurred at intervals of ~500 years at the end of Stage 2b.
3. Average magma discharge rates calculated from the tephra and lava products are 0.05 km^3/kyr (Stage 1), 2.9 km^3/kyr (Stage 2a), 0.07 km^3/kyr (Stage 2b), 1.1 km^3/kyr (Stage 3a; Miki and Kobayashi, 2016), and 4.0 km^3/kyr (Stage 3b).
4. The activity pattern of the Kitadake volcano changed around 8 ka; the rate of volcanic activity at Stage 2 declined after 8 ka. The aerial deposits developed above the P11 pumice fall deposits at 8 ka in outcrops on and around Sakurajima suggest the presence of repeated Vulcanian eruptions at Stage 2b.

Data availability statement

The original contributions presented in the study are included in the article/Supplementary Material, further inquiries can be directed to the corresponding author.

Author contributions

AN, NG, and HN conducted the field surveys and compiled the thickness data. NG and HN collected the charcoal samples for age determination. AN reconstructed the isopach contours and performed the volume calculation of each tephra. All authors contributed to data evaluation and interpretation.

Acknowledgments

This study is part of the Ph.D. thesis of AN. We appreciate Tetsuo Kobayashi for providing important information on the distribution of Sakurajima tephra deposits and for critical comments on the reexamined isopach contours. We also appreciate Katsuya Kaneko for reading the original draft and providing critical comments. We thank Christopher Conway for improving the manuscript. We thank Tatsuya Konoo for providing information on outcrops that are still observable and the thickness of Sakurajima tephras. We would like to thank the two reviewers for their critical comments which improved this manuscript.

Conflict of interest

The authors declare that the research was conducted in the absence of any commercial or financial relationships that could be construed as a potential conflict of interest.

Publisher's note

All claims expressed in this article are solely those of the authors and do not necessarily represent those of their affiliated organizations, or those of the publisher, the editors and the reviewers. Any product that may be evaluated in this article, or claim that may be made by its manufacturer, is not guaranteed or endorsed by the publisher.

Supplementary material

The Supplementary Material for this article can be found online at: https://www.frontiersin.org/articles/10.3389/feart.2022.988373/full#supplementary-material

References

Allan, A. S. R., Baker, J. A., Carter, L., and Wysoczanksi, R. J. (2008). Reconstructing the quaternary evolution of the world's most active silicic volcanic system: Insights from an ~1.65Ma deep ocean tephra record sourced from taupo volcanic zone, New Zealand. *Quat. Sci. Rev.* 27 (25), 2341–2360. doi:10.1016/j.quascirev.2008.09.003

Aramaki, S. (1984). formation of the Aira caldera, southern Kyushu, ~22, 000 years ago. *J. Geophys. Res.* 89 (B10), 8485–8501. doi:10.1029/JB089iB10p08485

Bonadonna, C., Biass, S., and Costa, A. (2015). Physical characterization of explosive volcanic eruptions based on tephra deposits: Propagation of uncertainties and sensitivity analysis. *J. Volcanol. Geotherm. Res.* 296, 80–100. doi:10.1016/j.jvolgeores.2015.03.009

Bonadonna, C., and Costa, A. (2012). Estimating the volume of tephra deposits: A new simple strategy. *Geology* 40 (5), 415–418. doi:10.1130/G32769.1

Bonadonna, C., and Houghton, B. (2005). Total grain-size distribution and volume of tephra-fall deposits. *Bull. Volcanol.* 67 (5), 441–456. doi:10.1007/s00445-004-0386-2

Daggitt, M. L., Mather, T. A., Pyle, D. M., and Page, S. (2014). AshCalc–a new tool for the comparison of the exponential, power-law and Weibull models of tephra deposition. *J. Appl. Volcanol.* 3 (1), 7–8. doi:10.1186/2191-5040-3-7

Donoghue, S. L., Neall, V. E., and Palmer, A. S. (1995). Stratigraphy and chronology of late Quaternary andesitic tephra deposits, Tongariro Volcanic Centre, New Zealand. *J. R. Soc. N. Z.* 25 (2), 115–206. doi:10.1080/03014223.1995.9517487

Fierstein, J., and Nathenson, M. (1992). Another look at the calculation of fallout tephra volumes. *Bull. Volcanol.* 54 (2), 156–167. doi:10.1007/BF00278005

Fukuyama, H. (1978). Geology of Sakurajima volcano, southern Kyushu. *Jour. Geol. Soc. Jpn.* 84 (6), 309–316. (in Japanese with English abstract). doi:10.5575/geosoc.84.309

Geshi, N., Yamada, I., Matsumoto, K., Nishihara, A., and Miyagi, I. (2020). Accumulation of rhyolite magma and triggers for a caldera-forming eruption of the Aira Caldera, Japan. *Bull. Volcanol.* 82 (6), 44–18. doi:10.1007/s00445-020-01384-6

Geshi, N., Oikawa, T., Weller, D. J., and Conway, C. E. (2022). Evolution of the magma plumbing system of Miyakejima volcano with periodic recharge of basaltic magmas. *Earth Planets Space* 74 (1), 20. doi:10.1186/s40623-022-01577-7

Greve, A., and Turner, G. M. (2017). New and revised palaeomagnetic secular variation records from post-glacial volcanic materials in New Zealand. *Phys. Earth Planet. Interiors* 269, 1–17. doi:10.1016/j.pepi.2017.05.009

Hayakawa, Y. (1985). Pyroclastic geology of Towada volcano. *Bull. Earthq. Res. Inst. Univ. Tokyo* 60 (4), 507–592. doi:10.15083/0000032881

Hayakawa, Y. (1993). A proposal of eruption magnitude scale. *Bull. Volcanol. Soc. Jpn.* 38 (6), 223–226. (in Japanese with English abstract). doi:10.18940/kazan.38.6_223

Hayashida, A., Yokota, K., and Yamada, K.Scientific Drilling Project Members (2022). Investigation of magnetic properties of the sediment core from Imuta-Ike Lake, Kagoshima Prefecture, using U-channel samples. *Chikyu monthly/special* 71, 107–111. (in Japanese).

Hiramine, H., Miyabuchi, Y., and Kobayashi, T. (2015). Description of outcrops for Take tephra located on the northern slope of Sakurajima volcano, southwest Japan : Implications for sequence of the last eruption at Kitadake Cone(<Special Section>Determination of the construction of an outcrop database to reveal eruptive history (2)). *Bull. Volcanol. Soc. Jpn.* 60 (2), 167–172. (in Japanese with English abstract). doi:10.18940/kazan.60.2_167

Ikuta, M., Niwa, M., Danhara, T., Yamashita, T., Maruyama, S., Kamataki, T., et al. (2016). Identification of pumice derived from historic eruption in the same volcano; Case study for the Sakurajima-Bunmei tephra in the Miyazaki Plain. *Jour. Geol. Soc. Jpn.* 122 (3), 2016.0003–107. (in Japanese with English abstract). doi:10.5575/geosoc.2016.0003

Inoue, Y., Nagatomo, Y., and Takaki, H. (1997). Identification of tephra deposits in the cumulative Andisols profile in Miyakonojo basin. *Pedologist* 41 (1), 42–54. (in Japanese with English abstract). doi:10.18920/pedologist.41.1_42

Ishihara, K., Takayama, T., Tanaka, Y., and Hirabayashi, J. (1981). Lava flow at Sakurajima Volcano. I: Volume of the historical lava flow. *Annu. Disas, Prev. Res. Inst., Kyoto Univ.* 24 (B-1), 1–10. (in Japanese with English abstract) Available at: http://hdl.handle.net/2433/70450.

Ishikawa, H., Higo, S., Tomari, Y., Oki, K., and Hamasaki, K. (1972). ^<14>C ages of the Kamou pumice flow and the Younger volcanic ash and pumice beds in the Kagoshima City, Kagoshima Prefecture. *Jour. Geol. Soc. Jpn.* 78 (10), 563–565. (in Japanese). doi:10.5575/geosoc.78.563

Iwamatsu, A., and Kobayashi, T. (1984). "Distribution and erosion of pumice fall deposits discharged by historical eruption in Sakurajima volcano," in *Research report of Sakurajima area scientific research council (2nd collection)*, 149–158. (in Japanese, English translation from the original title written in Japanese).

Kagoshima Prefecture (1999). "Report on the investigation of the Kagoshima bay west rim fault and the Izumi fault zone," in *Report on the results of the grant for earthquake-related basic research in 1998 fiscal year*. (in Japanese, English translation from the original title written in Japanese).

Kanai, M. (1920). "Research report on the sequence and products of the 1914 Sakurajima eruption and its impact on agriculture," in *Research reports on the 1914 Sakurajima eruption and its eruptive products* (Kagoshima-agricultural-high-school), 1–107. (in Japanese, English translation from the original title written in Japanese). doi:10.11501/959686

Kano, K., Yamamoto, T., and Ono, K. (1996). Subaqueous eruption and emplacement of the Shinjima pumice, Shinjima (moeshima) Island, Kagoshima bay, SW Japan. *J. Volcanol. Geotherm. Res.* 71 (2-4), 187–206. doi:10.1016/0377-0273(95)00077-1

Kano, K., Yanagisawa, Y., Okuno, M., Nakagawa, M., Uchimura, K., Miki, D., et al. (2022). Post-caldera volcanism and environmental changes in Aira caldera, inner Kagoshima bay, SW Japan. *Jour. Geol. Soc. Jpn.* 128 (1), 2022.0003–62. (in Japanese with English abstract). doi:10.5575/geosoc.2022.0003

Kobayashi, T. (1982). Geology of Sakurajima volcano : A review. *SECOND Ser. Bull. Volcanol. Soc. Jpn.* 27 (4), 277–292. (in Japanese with English abstract). doi:10.18940/kazanc.27.4_277

Kobayashi, T. (1986a). "Volcanic ash deposits formed by the intermittent eruptions of the active volcano Sakurajima," in *Reports of the reference center of the scientific researches for southwest pacific area* (Kagoshima University, Special Volume 1), 1–12. (in Japanese with English abstract).

Kobayashi, T. (1986b). *Volcanic history and pyroclastic flows of Sakurajima Volcano*. Reports for Grants-in-Aid for Research in Natural Disasters (no. 58020012), characteristics of dry high concentration flows (pyroclastic flows etc.) associated with volcanic eruption and their disasters. Principal Investigator: S. Aramaki, 137–163. (in Japanese).

Kobayashi, T. (1989). "Eruptions during initial stage of Sakurajima Volcano and their radiocarbon ages,". *Abstract retrieved from abstracts of papers presented at the spring meeting of the society in second series bulletin of the volcanological society of Japan*, 34, 130. (in Japanese). doi:10.18940/kazanc.34.2_130_1

Kobayashi, T. (2010). "Formation age of nakadake of Sakurajima volcano : Was it formed in historical time ?,". *Abstract retrieved from PROGRAMME AND ABSTRACTS THE VOLCANOLOGICAL SOCIETY OF Japan*, 2010, 33. (in Japanese). doi:10.18940/vsj.2010.0_33

Kobayashi, T., and Ezaki, M. (1996). "Eruptive history of Sakurajima volcano, southern Kyushu, Japan,". *Summaries of researchers using AMS at nagoya university*, 7, 70–81. (in Japanese with English abstract).

Kobayashi, T., and Ezaki, M. (1997). Reexamination of eruptive history of Sakurajima volcano. *Chikyu Mon.* 19 (4), 227–231. (in Japanese, English translation from the original title written in Japanese).

Kobayashi, T., and Tameike, T. (1999). "Thickness and grain-size distribution of the Satsuma tephra from Sakurajima volcano," in *Reports for grants-in-aid for general scientific research (no. 04680248) from ministry of education*. Editor H. Miyamachi (Principal Investigator), 31–97. (in Japanese, English translation from the original title written in Japanese).

Kobayashi, T., and Tameike, T. (2002). History of eruptions and volcanic damage from Sakurajima volcano, southern Kyushu, Japan. *Daiyonki-kenkyu.* 41 (4), 269–278. (in Japanese with English abstract). doi:10.4116/jaqua.41.269

Kobayashi, T., Okuno, M., Nakamura, T., and Fukushima, D. (2009). "Newly discovered historic lava flow from Minamidake, Sakurajima volcano,". *Abstract retrieved from PROGRAMME AND ABSTRACTS THE VOLCANOLOGICAL SOCIETY OF Japan*, 2009, 164. (in Japanese). doi:10.18940/vsj.2009.0_164

Kobayashi, T., Miki, D., Sasaki, H., iguchi, M., Yamamoto, T., and Uto, K. (2013). *Geological map of Sakurajima volcano (2nd ed.)*. Geological Survey of Japan, AIST.

Kuwahata, M., Sugiyama, S., Nakanishi, T., Adachi, T., Tajiri, Y., Shimoyama, S., et al. (2021). Environmental change before and after the kikai-akahoya tephra: Examination of teh MIK core analysis, miazaki plain, southeastern Kyushu. *Chikyu monthly/special* 70, 89–99. (in Japanese).

Leonard, G. S., Cole, R. P., Christenson, B. W., Conway, C. E., Cronin, S. J., Gamble, J. A., et al. (2021). Ruapehu and tongariro stratovolcanoes: A review of current understanding. *New zeal. J. Geol. geophys.* 64 (2-3), 389–420. doi:10.1080/00288306.2021.1909080

Lowe, D. J., and Hunt, J. B. (2001). A summary of terminology used in tephra-related studies. *Tephra Les Dossiers l'Archeo-Logis* 1, 17–22.

Machida, H., and Arai, F. (1978). Akahoya ash-A holocene widespread tephra erupted from the Kikai caldera, south Kyushu, Japan. *Daiyonki-kenkyu*. 17 (3), 143–163. (in Japanese with English abstract). doi:10.4116/jaqua.17.143

Machida, H., Ota, Y., Kawana, T., Moriwaki, H., and Nagaoka, S. (2001). *Regional geomorphology of the Japanese Island vol. 7 geomorphology of Kyushu and the ryukyus*. University of Tokyo Press.

Matumoto, T. (1943). The four gigantic caldera volcanoes of Kyushu. *Jpn. J. Geol. Geog.* 19, 1–57.

Miki, D. (1999). Estimate of the ages of lava flows at Sakurajima volcano, Kyushu, Japan; inferred from paleomagnetic directions and paleointensities. *Bull. Volcanol. Soc. Jpn.* 44 (3), 111–122. (in Japanese with English abstract). doi:10.18940/kazan.44.3_111

Miki, D., and Kobayashi, T. (2016). the formation process of Minamidake edifice on Sakurajima volcano, Japan : As inferred from paleomagnetic age of lavas and volume of volcanic products. *Bull. Volcanol. Soc. Jpn.* 61 (1), 237–252. (in Japanese with English abstract). doi:10.18940/kazan.61.1_237

Miki, D., Uto, K., Uchiumi, S., and Ishihara, K. (2000). K-Ar dating and paleomagnetic measurements on drilled cores from the Sakurajima volcano: Part 2. *Annu. Disas. Prev. Res. Inst. Kyoto Univ.*, 1–6. (in Japanese with English abstract) Available at: http://hdl.handle.net/2433/80465.

Miki, D., Uto, K., Sudo, M., and Ishihara, K. (2003). Correlation of lavas on drilled cores from the Sakurajima volcano, inferred from paleomagnetic and chemical features. *Annu. Disas, Prev. Res. Inst., Kyoto Univ.* 46, 835–840. (in Japanese with English abstract) Available at: http://hdl.handle.net/2433/129104.

Miki, D., Uto, K., Hoang, N., and Ishihara, K. (2012). Age of lava flows in southwestern slope of Minamidake, Sakurajima volcano, inferred from paleomagnetic and chemical features. *Annu. Disas, Prev. Res. Inst., Kyoto Univ.* 55 (B), 177–181. Available at: http://hdl.handle.net/2433/161856.

Miyabuchi, Y. (2009). A 90, 000-year tephrostratigraphic framework of Aso Volcano, Japan. *Sediment. Geol.* 220 (3), 169–189. doi:10.1016/j.sedgeo.2009.04.018

Moriwaki, H. (1990). "Late pleistocene big eruption of Sakurajima volcano: Satsuma tephra eruption," in *Reports of the reference center of the scientific researches for southwest pacific area* (Kagoshima University, Special Volume 3), 40–47. (in Japanese with English abstract).

Moriwaki, H. (1992). Late Quaternary phreatomagmatic tephra layers and their relation to paleo-sea levels in the area of Aira caldera, southern Kyushu, Japan. *Quat. Int.* 13, 195–200. doi:10.1016/1040-6182(92)90028-Z

Moriwaki, H. (1994). "Palaeoenvironmental study on late quaternary fine ash beds around Kagoshima bay," in *Reports for grants-in-aid for scientific research (no. 04680248) from ministry of education*. Editor H. Moriwaki (Principal Investigator), 1–20. (in Japanese, English translation from the original title written in Japanese).

Moriwaki, H. (2010). "Late pleistocene and holocene tephras in southern Kyushu," in *Intra-conference field trip guides. INTAV international field conference and workshop on tephrochronology, volcanism, and human activity, Kirishima city, Kyushu, Japan*. Editors H. Moriwaki and D. J. Lowe, 44–53.

Moriwaki, H., Machida, H., Hatsumi, Y., and Matsushima, Y. (1986). Phreatomagmatic eruptions affected by postglacial transgression in the northern coastal area of Kagoshima bay, southern Kyushu, Japan. *J. Geogr. (Chigaku Zasshi)* 95 (2), 94–113. (in Japanese with English abstract). doi:10.5026/jgeography.95.2_94

Moriwaki, H., Suzuki, T., Murata, M., Ikehara, M., Machida, H., and Lowe, D. J. (2011). Sakurajima-satsuma (Sz-S) and noike-yumugi (N-ym) tephras: New tephrochronological marker beds for the last deglaciation, southern Kyushu, Japan. *Quat. Int.* 246 (1-2), 203–212. doi:10.1016/j.quaint.2011.03.046

Moriwaki, H., Matsushima, Y., Sugihara, S., Ohira, A., Oki, K., Masubuchi, K., et al. (2015). Sea-level and palaeoenvironmental changes of Kokubu plain on the northern coast of Kagoshima Bay, south Japan, since 15, 000 years ago. *Daiyonki-kenkyu.* 54 (4), 149–171. (in Japanese with English abstract). doi:10.4116/jaqua.54.149

Moriwaki, H., Nakamura, N., Nagasako, T., Lowe, D. J., and Sangawa, T. (2016). The role of tephras in developing a high-precision chronostratigraphy for palaeoenvironmental reconstruction and archaeology in southern Kyushu, Japan, since 30, 000 cal. BP: An integration. *Quat. Int.* 397, 79–92. doi:10.1016/j.quaint.2015.05.069

Moriwaki, H., Nagasako, T., Nishizawa, F., Matsushima, Y., Suzuki, T., and Tanaka, G. (2017). Chronology and significance of marine deposits on Shinjima (moeshima) Island, Kagoshima bay, based on tephrochronology and ^{14}C ages. *J. Geogr. Zasshi).* 126 (5), 557–579. (in Japanese with English abstract). doi:10.5026/jgeography.126.557

Nagasako, T., Okuno, M., Moriwaki, H., Arai, F., and Nakamura, T. (1999). Paleogeography and tephras of the Kimotsuki lowland, southern Kyushu, Japan, in the middle to late Holocene. *Daiyonki-kenkyu.* 38 (2), 163–173. (in Japanese with English abstract). doi:10.4116/jaqua.38.163

Nakamura, K. (2006). Textures of plagioclase microlite and vesicles within volcanic products of the 1914-1915 eruption of Sakurajima Volcano, Kyushu, Japan. *J. Mineralogical Petrological Sci.* 101 (4), 178–198. doi:10.2465/jmps.101.178

Naruo, H., and Geshi, N. (2020). "Geology of kasugabori site," in *Reports of Kagoshima prefecture cultural promotion foundation, archaeological research center, No.32, Kasugabori site 1*. Editors M. Kawaguchi, E. Kinoshita, S. Fukunaga, and R. Magome, 194–201. (in Japanese, English translation from the original title written in Japanese). doi:10.24484/sitereports.72344

Naruo, H., and Kobayashi, T. (1984). "Pyroclastic fall deposits from Ikeda caldera,". Abstract retrieved from *abstracts of papers presented at the spring meeting of the society in second series bulletin of the volcanological society of Japan*, 29, 148. (in Japanese, English translation from the original title written in Japanese). doi:10.18940/kazanc.29.2_148_22

Naruo, H. (1991). Validity of tephra erupted during the early Jomon period in southern Kyushu. *NEWS Lett. JOMON STUDY* 4, 33–40. (in Japanese, English translation from the original title written in Japanese). doi:10.11501/4426155

Newhall, C. G., and Self, S. (1982). The volcanic explosivity index (VEI) an estimate of explosive magnitude for historical volcanism. *J. Geophys. Res.* 87 (C2), 1231–1238. doi:10.1029/JC087iC02p01231

Nishihara, A., Geshi, N., and Naruo, H. (2022). "The tephra deposits of Sakurajima volcano described in archeological sites, No. 1," in *Open-file report of the geological survey of Japan, AIST, no.737*. (in Japanese with English abstract). Available at: https://www.gsj.jp/publications/pub/openfile/openfile0737.html.

Nishimura, K., and Kobayashi, T. (2015). Chemical characteristics of Takano base surge deposit and Shinjima pumice from Aira Caldera, SW Japan. *Chikyu Mon.* 37, 259–264. (in Japanese).

Obrochta, S. P., Yokoyama, Y., Yoshimoto, M., Yamamoto, S., Miyairi, Y., Nagano, G., et al. (2018). Mt. Fuji Holocene eruption history reconstructed from proximal lake sediments and high-density radiocarbon dating. *Quat. Sci. Rev.* 200, 395–405. doi:10.1016/j.quascirev.2018.09.001

Okuno, M. (2002). Chronology of tephra layers in southern Kyushu, SW Japan, for the last 30, 000 years. *Daiyonki-kenkyu.* 41 (4), 225–236. (in Japanese with English abstract). doi:10.4116/jaqua.41.225

Okuno, M., Nakamura, T., Moriwaki, H., and Kobayashi, T. (1997). AMS radiocarbon dating of the Sakurajima tephra group, southern Kyushu, Japan. *Nucl. Instrum. Methods Phys. Res. Sect. B Beam Interact. Mater. Atoms* 123 (1-4), 470–474. doi:10.1016/S0168-583X(96)00614-3

Okuno, M., Tameike, T., Naruo, H., Moriwaki, H., Nakamura, T., and Kobayashi, T. (1999). Eruptive age of Sakurajima P13 tephra (Sz-P13)- insight from accelerator

^{14}C dating of buried soil samples-. *Kagoshima J. Archaeol.* 33, 95–102. (in Japanese, English translation from the original title written in Japanese).

Óladóttir, B. A., Sigmarsson, O., Larsen, G., and Thordarson, T. (2008). Katla volcano, Iceland: Magma composition, dynamics and eruption frequency as recorded by holocene tephra layers. *Bull. Volcanol.* 70 (4), 475–493. doi:10.1007/s00445-007-0150-5

Pyle, D. M. (1995). Mass and energy budgets of explosive volcanic eruptions. *Geophys. Res. Lett.* 22 (5), 563–566. doi:10.1029/95GL00052

Pyle, D. M. (1989). The thickness, volume and grainsize of tephra fall deposits. *Bull. Volcanol.* 51 (1), 1–15. doi:10.1007/BF01086757

Ramsey, C. B. (2009). Bayesian analysis of radiocarbon dates. *Radiocarbon* 51 (1), 337–360. doi:10.1017/S0033822200033865

Reimer, P. J., Austin, W. E., Bard, E., Bayliss, A., Blackwell, P. G., Ramsey, C. B., et al. (2020). The IntCal20 Northern Hemisphere radiocarbon age calibration curve (0–55 cal kBP). *Radiocarbon* 62 (4), 725–757. doi:10.1017/RDC.2020.41

Sagawa, T., Nagahashi, Y., Satoguchi, Y., Holbourn, A., Itaki, T., Gallagher, S. J., et al. (2018). Integrated tephrostratigraphy and stable isotope stratigraphy in the Japan sea and east China sea using IODP sites U1426, U1427, and U1429, expedition 346 asian monsoon. *Prog. Earth Planet. Sci.* 5 (1), 18. doi:10.1186/s40645-018-0168-7

Smith, V. C., Staff, R. A., Blockley, S. P. E., Bronk Ramsey, C., Nakagawa, T., Mark, D. F., et al. (2013). Identification and correlation of visible tephras in the lake suigetsu SG06 sedimentary archive, Japan: Chronostratigraphic markers for synchronising of east asian/west pacific palaeoclimatic records across the last 150 ka. *Quat. Sci. Rev.* 67, 121–137. doi:10.1016/j.quascirev.2013.01.026

Soda, T. (1997). "Volcanic ash deposits and formation of soil," in *The history of Miyazaki prefecture: Series of comprihensive history 1 (the primitive age and the ancient time (1))* (Miyazaki-prefecture), 33–77. (in Japanese, English translation from the original title written in Japanese).

Sudo, M., Uto, K., Miki, D., and Ishihara, K. (2001). K-Ar dating of volcanic rocks along the Aira caldera rim: Part 2: Volcanic history of Western and northwestern area of caldera and Sakurajima volcano. *Annu. Disas, Prev. Res. Inst., Kyoto Univ.* 44 (B-1), 305–316. (in Japanese with English abstract). Available at: http://hdl.handle.net/2433/80514.

Sun, C., Wang, L., Plunkett, G., Zhang, E., and Liu, J. (2021). An integrated late pleistocene to holocene tephrostratigraphic framework for south-east and east asia. *Geophys. Res. Lett.* 48 (5), e2020GL090582. doi:10.1029/2020GL090582

Sunyé-Puchol, I., Hodgetts, A. G. E., Watt, S. F. L., Arce, J. L., Barfod, D. N., Mark, D. F., et al. (2022). Reconstructing the middle to late Pleistocene explosive eruption histories of Popocatépetl, Iztaccíhuatl and Tláloc-Telapón volcanoes in Central México. *J. Volcanol. Geotherm. Res.* 421, 107413. doi:10.1016/j.jvolgeores.2021.107413

Szakács, A., Cañón-Tapia, E., and Szakács, A. (2010). "Some challenging new perspectives of volcanology," in *What is a volcano?* Editors E. Cañón-Tapia and A. Szakács (Geological Society of America), 123–140. doi:10.1130/2010.2470(09

Takahashi, M., Otsuka, T., Sako, H., Kawamata, H., Yasui, M., Kanamaru, T., et al. (2013). Temporal variation for magmatic chemistry of the Sakurajima volcano and Aira caldera region, southern Kyushu, southwest Japan since 61 ka and its implications for the evolution of magma chamber system (< special Section> Sakurajima special issue). *Bull. Volcanol. Soc. Jpn.* 58 (1), 19–42. doi:10.18940/kazan.58.1_19

Tatsumi, Y., Suzuki-Kamata, K., Matsuno, T., Ichihara, H., Seama, N., Kiyosugi, K., et al. (2018). Giant rhyolite lava dome formation after 7.3 ka supereruption at Kikai caldera, SW Japan. *Sci. Rep.* 8 (1), 2753. doi:10.1038/s41598-018-21066-w

Todde, A., Cioni, R., Pistolesi, M., Geshi, N., and Bonadonna, C. (2017). The 1914 taisho eruption of Sakurajima volcano: Stratigraphy and dynamics of the largest explosive event in Japan during the twentieth century. *Bull. Volcanol.* 79 (10), 72–22. doi:10.1007/s00445-017-1154-4

Tsukui, M. (2011). Ash-fall distribution of 1779 an'ei eruption, Sakurajima volcano : Revealed by historical documents. *Bull. Volcanol. Soc. Jpn.* 56 (2-3), 89–94. (in Japanese with English abstract). doi:10.18940/kazan.56.2-3_89

Tsuyuki, T. (1969). Geological study of hot springs in Kyushu, Japan(5) some hot springs in the Kagoshima graben, with special reference to thermal water reservoir. *Rep. Fac . Sci. Kagoshima Univ. Geol. Biol.* 2, 85–101. (in Japanese with English abstract) Available at: http://hdl.handle.net/10232/5842.

Umeda, K., Ban, M., Hayashi, S., and Kusano, T. (2013). Tectonic shortening and coeval volcanism during the Quaternary, Northeast Japan arc. *J. Earth Syst. Sci.* 122 (1), 137–147. doi:10.1007/s12040-012-0245-z

Uto, K., Miki, D., Uchiumi, S., and Ishihara, K. (1999). K-Ar dating and paleomagetic measurements on drilled cores from the Sakurajima volcano: Preliminary attempts to reveal the history of the volcanic activity. *Annu. Disas, Prev. Res. Inst., Kyoto Univ.* 42, 27–34. (in Japanese with English abstract) Available at: http://hdl.handle.net/2433/80399.

Uto, K., Miki, D., Hoang, N., Sudo, M., Fukushima, D., and Ishihara, K. (2005). Temporal evolution of magma composition in Sakurajima volcano, southwest Japan. *Annu. Disas, Prev. Res. Inst., Kyoto Univ.* 48 (B), 341–347. (in Japanese with English abstract) Available at: http://hdl.handle.net/2433/26514.

Yamamoto, T., Geshi, N., and Kobayashi, T. (2013). Geochemical features of pyroclastic deposits in the yokoyama core, Sakurajima volcano, SW Japan. *Bull. Volcanol. Soc. Jpn.* 58 (4), 519–528. (in Japanese with English abstract). doi:10.18940/kazan.58.4_519

Yamamoto, T., Kudo, T., and Isizuka, O. (2018). Temporal variations in volumetric magma eruption rates of Quaternary volcanoes in Japan. *Earth Planets Space* 70 (1), 65. doi:10.1186/s40623-018-0849-x

Paleoenvironment Research Institute (2002). "Soil horizon and tephra in Toudi Taguchi A site," in *Cultural series of kumamoto prefecture, No. 206, toudi taguchi A site*. Editor T. Yamashiro, 187–190. (in Japanese, English translation from the original title written in Japanese). doi:10.24484/sitereports.15599

Zernack, A. V., Cronin, S. J., Neall, V. E., and Procter, J. N. (2011). A medial to distal volcaniclastic record of an andesite stratovolcano: Detailed stratigraphy of the ring-plain succession of south-west taranaki, New Zealand. *Int. J. Earth Sci.* 100 (8), 1937–1966. doi:10.1007/s00531-010-0610-6